Notions of poromechanics in earthquake and faulting phenomena

Luca Dal Zilio

Theory of poroelasticity

The simultaneous deformation of the porous material and the flow of the pore fluid is the subject of the theory of consolidation, often denoted as **poroelasticity**.

The theory was developed originally by Terzaghi (1923, 1925) for the one-dimensional case, and extended to three dimensions by Biot (1941), and it has been studied extensively since.

The basic principles of the theory of poroelasticity are twofold: the equations of equilibrium of the porous medium, and the equations of conservation of mass of the two components: the solids and the pore fluid. It is convenient to start by considering the influence of the compressibilities of the two constituents on the behaviour of a porous medium in the absence of drainage.

Theory of poroelasticity

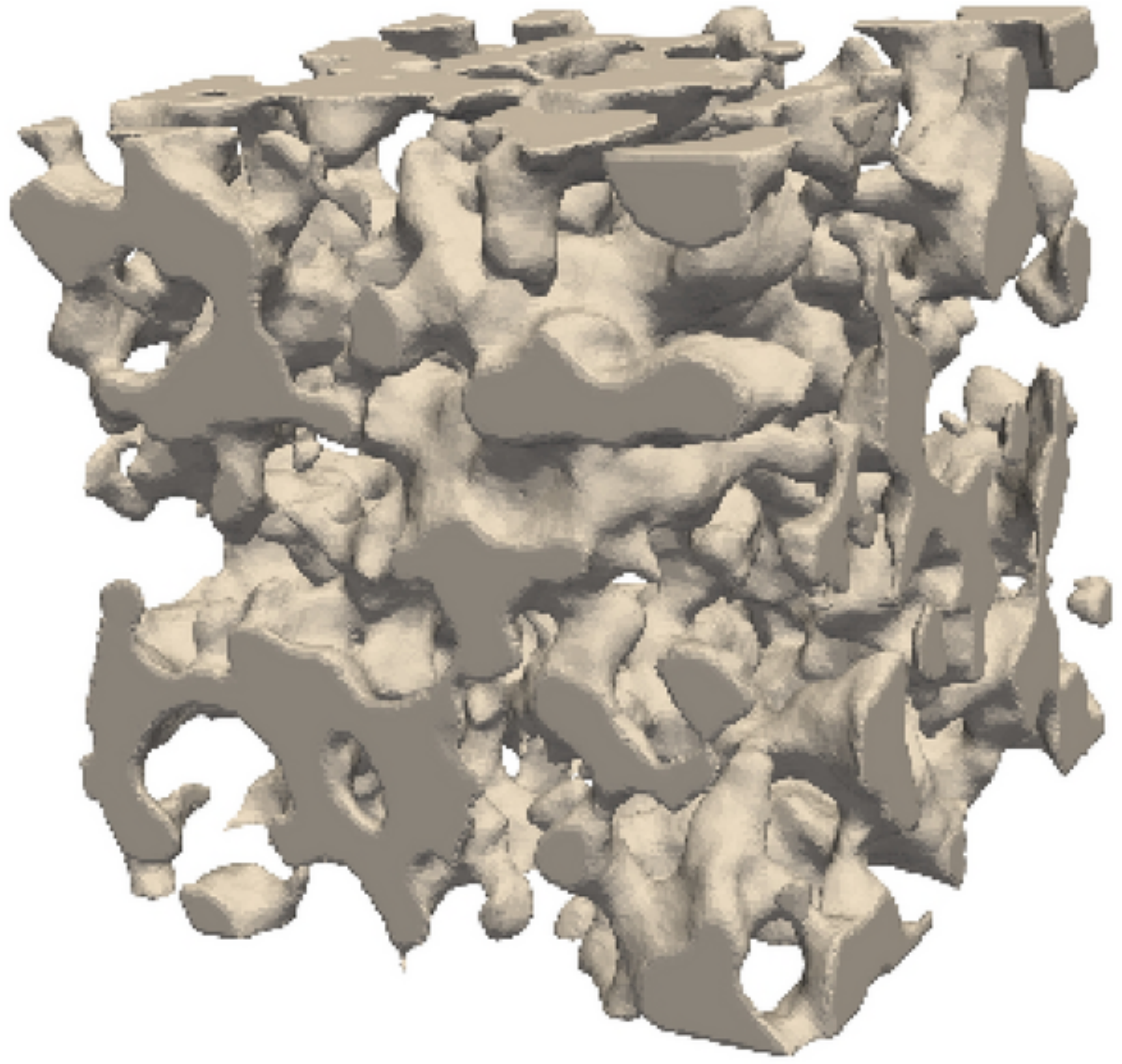

Why poroelasticity matter?

We often consider the earth's crust to be a solid nonporous elastic, or viscoelastic, medium. In actuality, the crust is porous and, except for the very shallow near-surface region, at least partially liquid saturated.

That rock is a multiphase composite consisting of solid and liquid filled pores adds a significant richness to its mechanical behavior. The liquid phase flows under gradients in pore-fluid pressure. Changes in fluid pressure induce strains, and conversely, changes in stress or strain induce changes in pore pressure.

Theory of poroelasticity

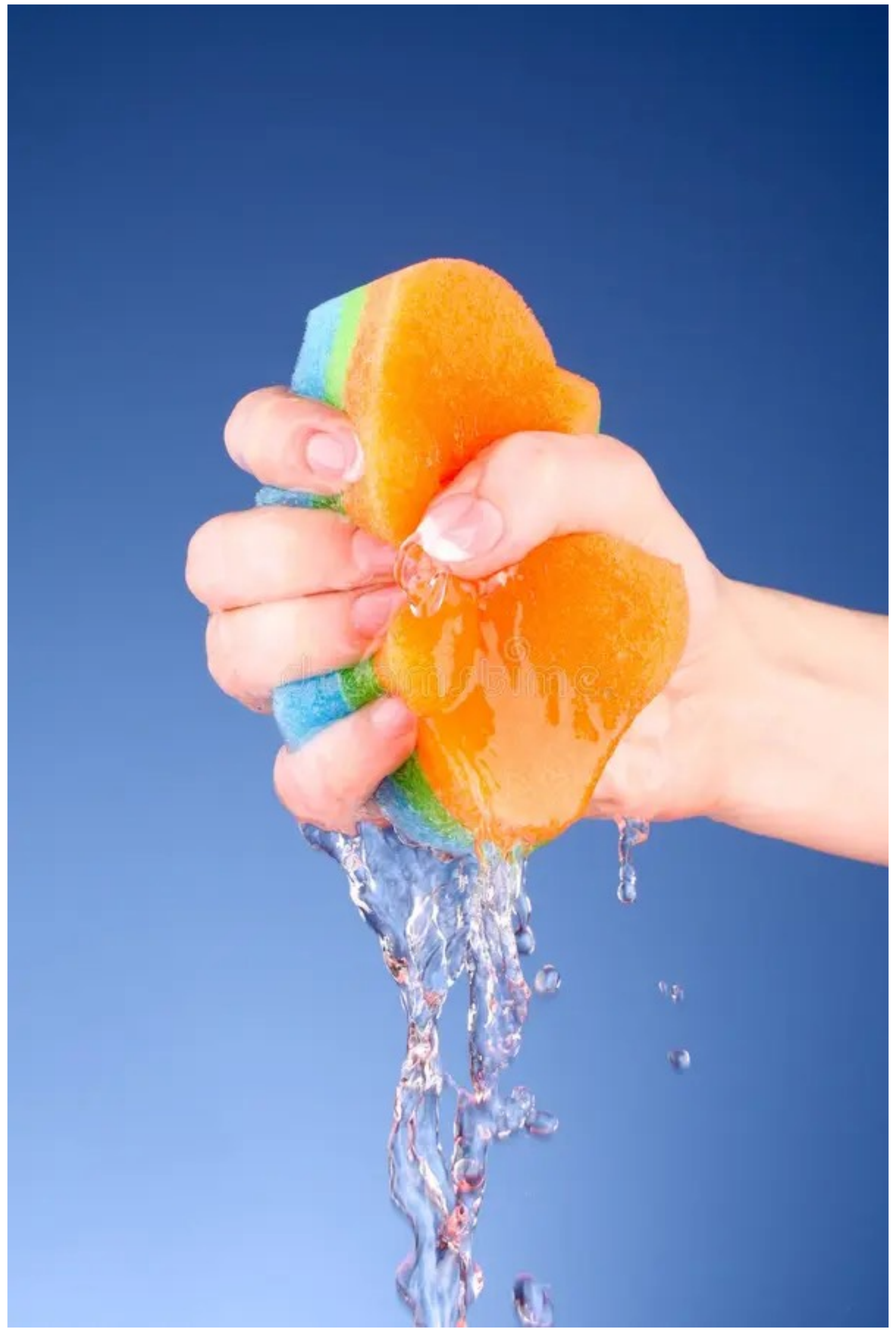

To see this at an intuitive level, consider a fluid-saturated sponge. Rapidly squeezing the sponge compacts the pore space and causes the pressure of the water in the pores to rise. The converse is that decreasing the water content by allowing the sponge to dry causes the sponge to shrink.

This duality has important geophysical implications…

Theory of poroelasticity

Because fluid pressure responds to strain, measuring pore-pressure changes in wells can be used to infer strain changes in the earth. In effect, water wells in confined aquifers can be employed as strain-meters.

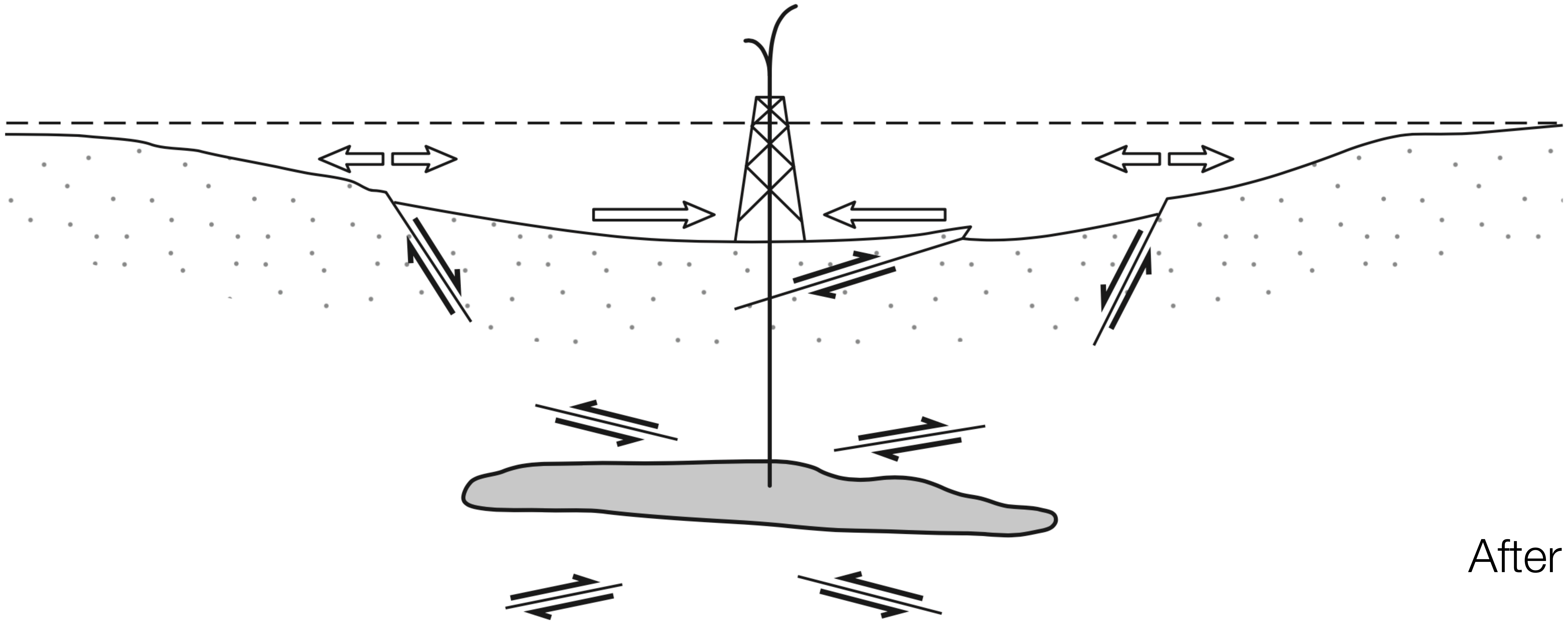

After Segall (1989)

Changes in fluid pressure cause deformation is apparent in many places where large volumes of fluid have been extracted from subsurface reservoirs. **Variations in fluid pressure also lead to more subtle deformations that in some cases can be misinterpreted as tectonic or volcanic in origin.**

Undrained compression of a porous medium

Isotropic total stress Δσ, in undrained condition, i.e. with no fluid flowing into or out of the element

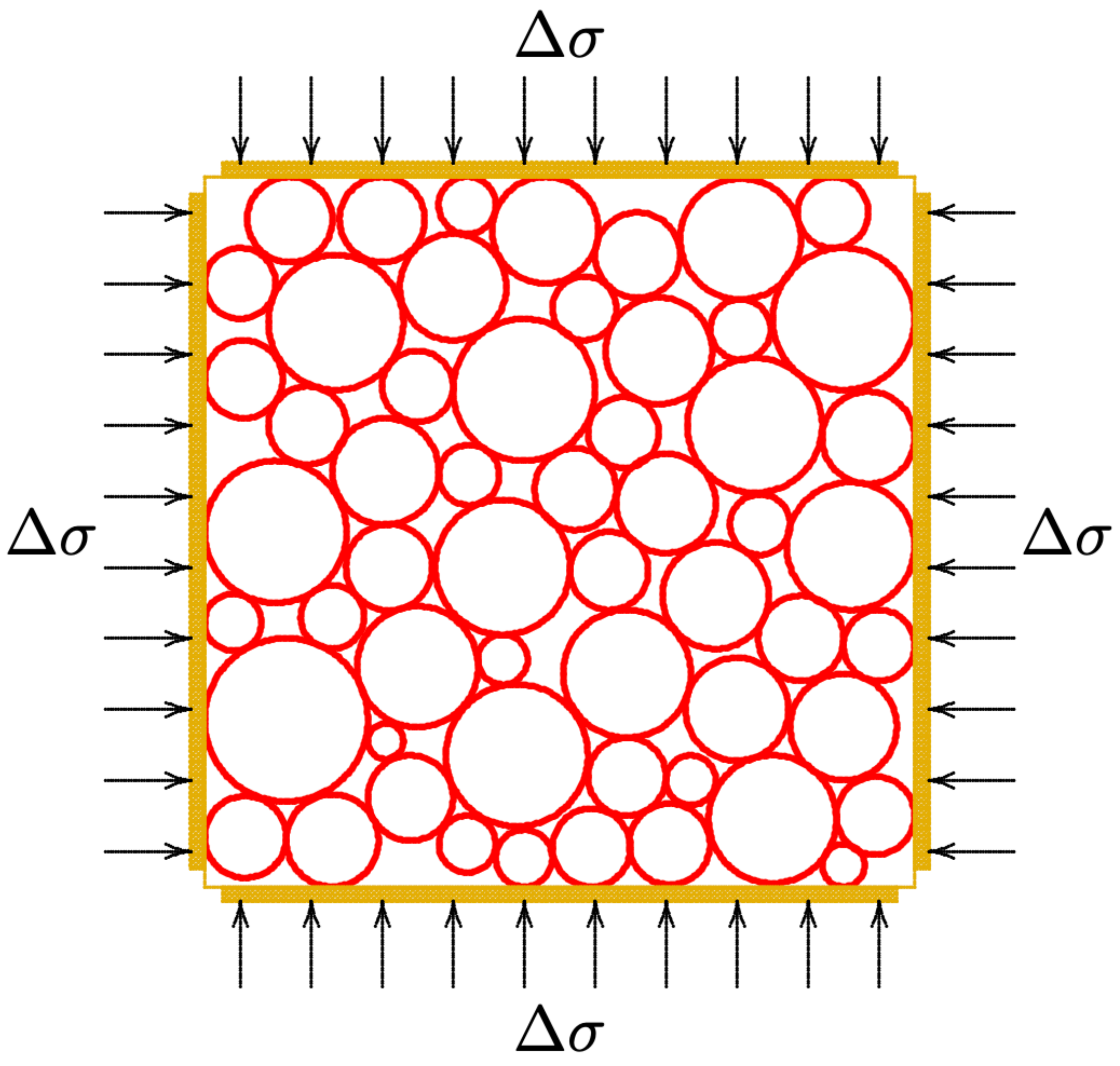

Let there be considered an element of porous soil or rock, of porosity n, saturated with a fluid, where the porosity is defined as the volume of the pores per unit total volume of the soil.

The resulting pore pressure (the pressure in the pore fluid) is denoted by Δp. In order to determine the relation between Δp and Δσ, we assume an increment of pressure both in the fluid and in the solid particles of magnitude Δp

Undrained compression of a porous medium

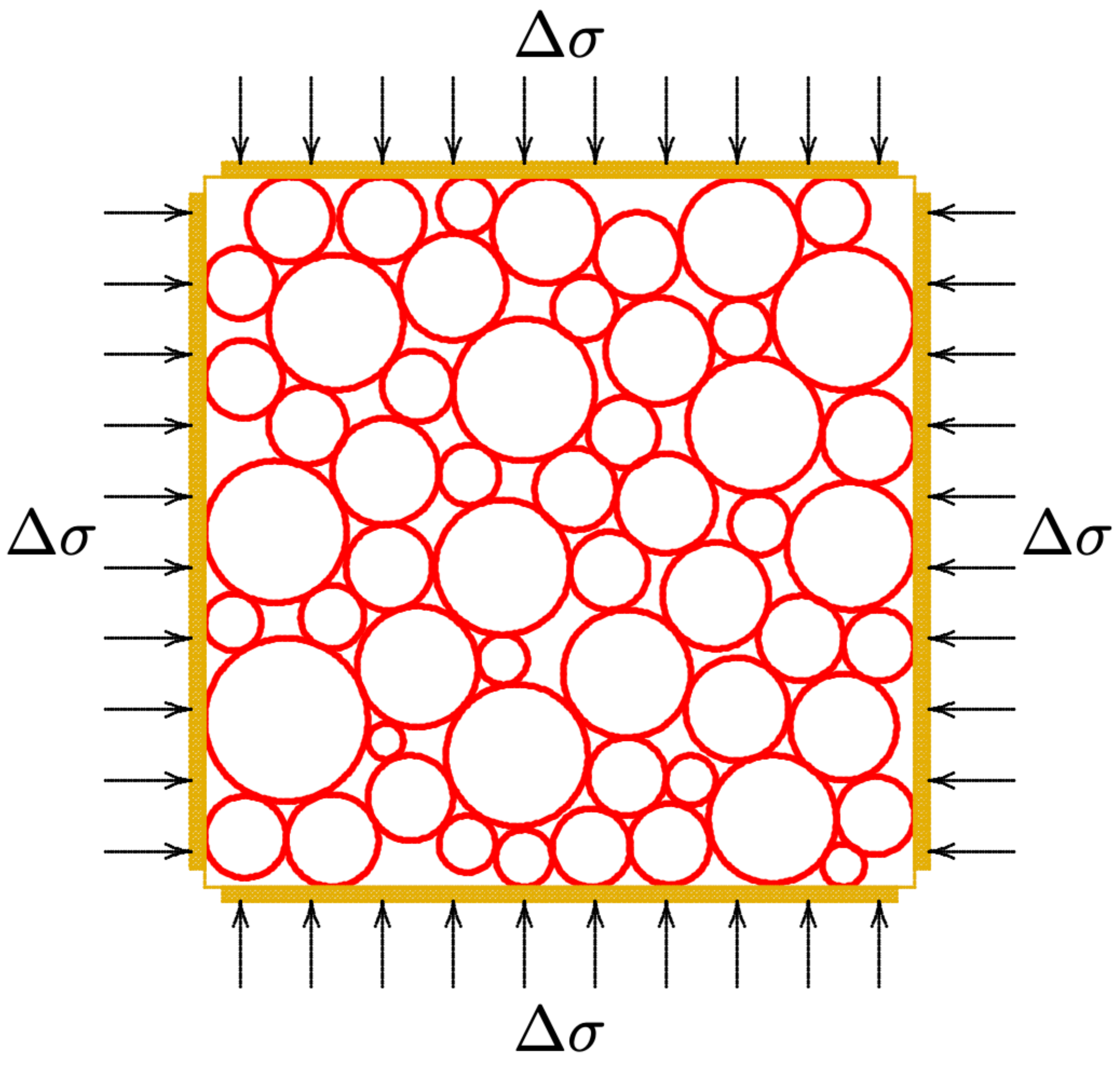

Assuming the stress in both fluid and particles is increased by Δp, the volume change of the pore fluid is:

$$\Delta V_f = -nC_f \Delta p V,$$

The volume change of the particles is, because the original volume of the particles is (1–n) V

$$\Delta V_s = -(1-n)C_s \Delta p V,$$

Assuming that the solid particles all have the same compressibility, it follows that their uniform compression leads to a volume change of the pore space:

$$\Delta V = -C_s \Delta p V$$

Undrained compression of a porous medium

The coefficient *B* can easily be determined experimentally by performing an undrained triaxial test (Bishop & Henkel, 1962).

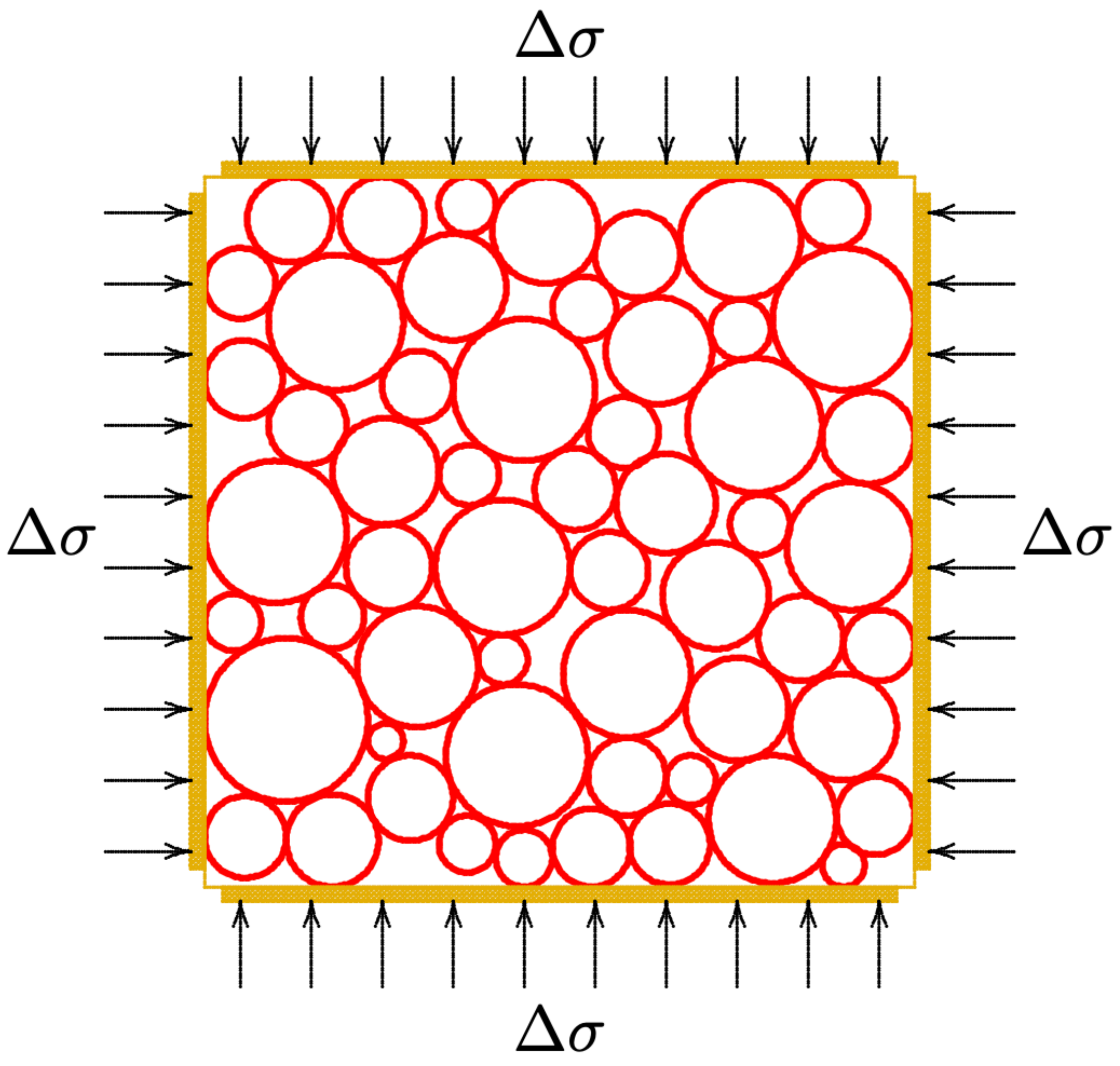

Because there is no drainage, by assumption, the total volume change must be equal to the sum of the volume changes of the fluid and the particles. This gives:

$$\frac{\Delta p}{\Delta \sigma} = B = \frac{1}{1 + n(C_f - C_s)/(C_m - C_s)}$$

$$= \frac{C_m - C_s}{(C_m - C_s) + n(C_f - C_s)},$$

The derivation leading to this equation is due to Bishop (1973) and earlier by Gassmann (1951). The ratio $\Delta p/\Delta\sigma$ under isotropic loading is often denoted by *B* in soil mechanics (Skempton, 1954). In that case *B* = 1, which is sometimes used as a first approximation in soil mechanics.

The principle of effective stress

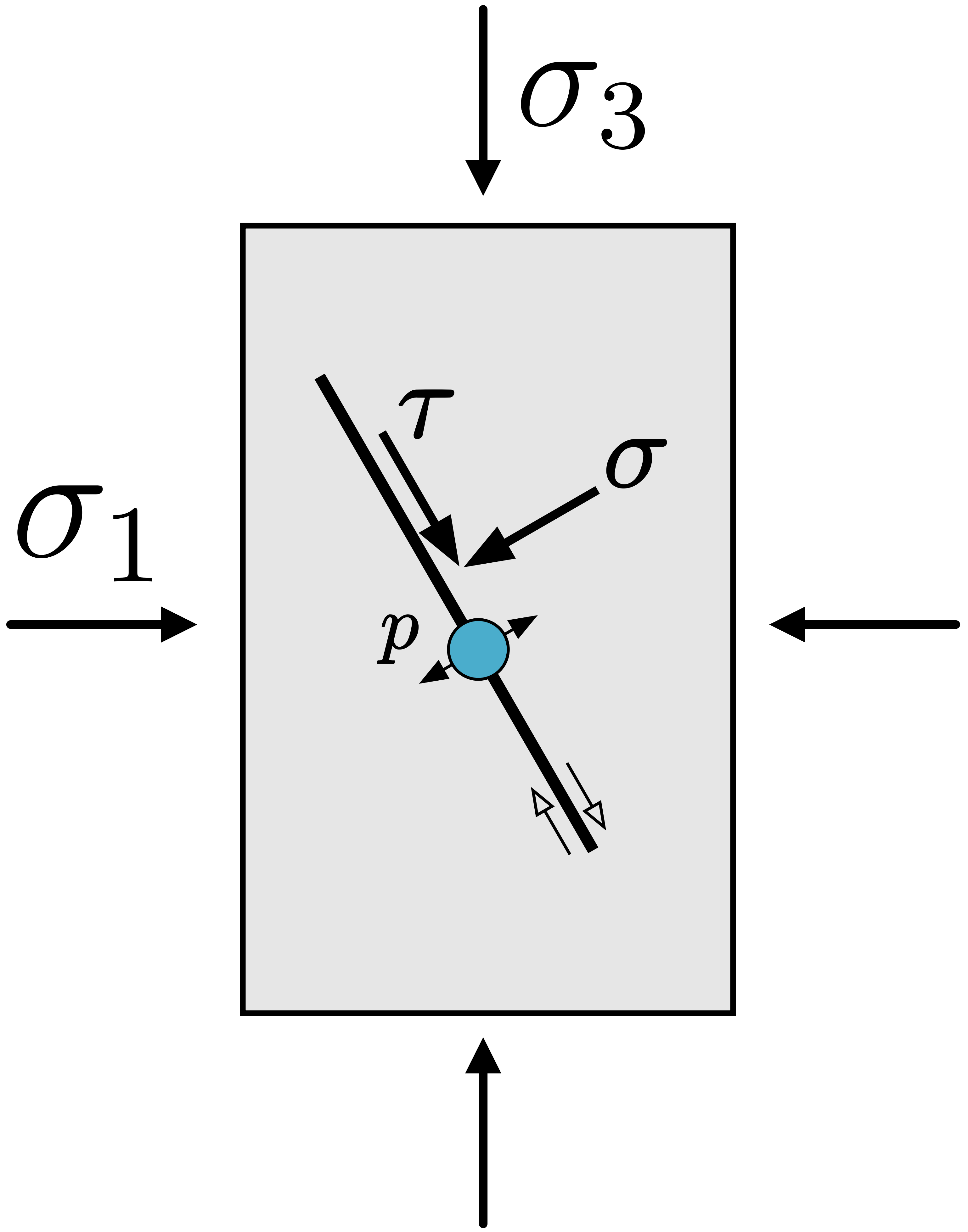

The effective stress, introduced by Terzaghi (1923, 1925), is defined as that part of the total stresses that governs the deformation of the soil or rock. It is assumed that the total stresses can be decomposed into the sum of the effective stresses and the pore pressure by writing

$$\sigma_{ij} = \sigma'_{ij} + \alpha p \delta_{ij}$$

where σ are the components of total stress, σ' are the components of effective stress, p is the pore pressure (the pressure in the fluid in the pores), δ are the Kronecker delta symbols (δ = 1 if i = j and δ = 0 otherwise), and **α is Biot's coefficient, which is unknown at this stage**.

The principle of effective stress

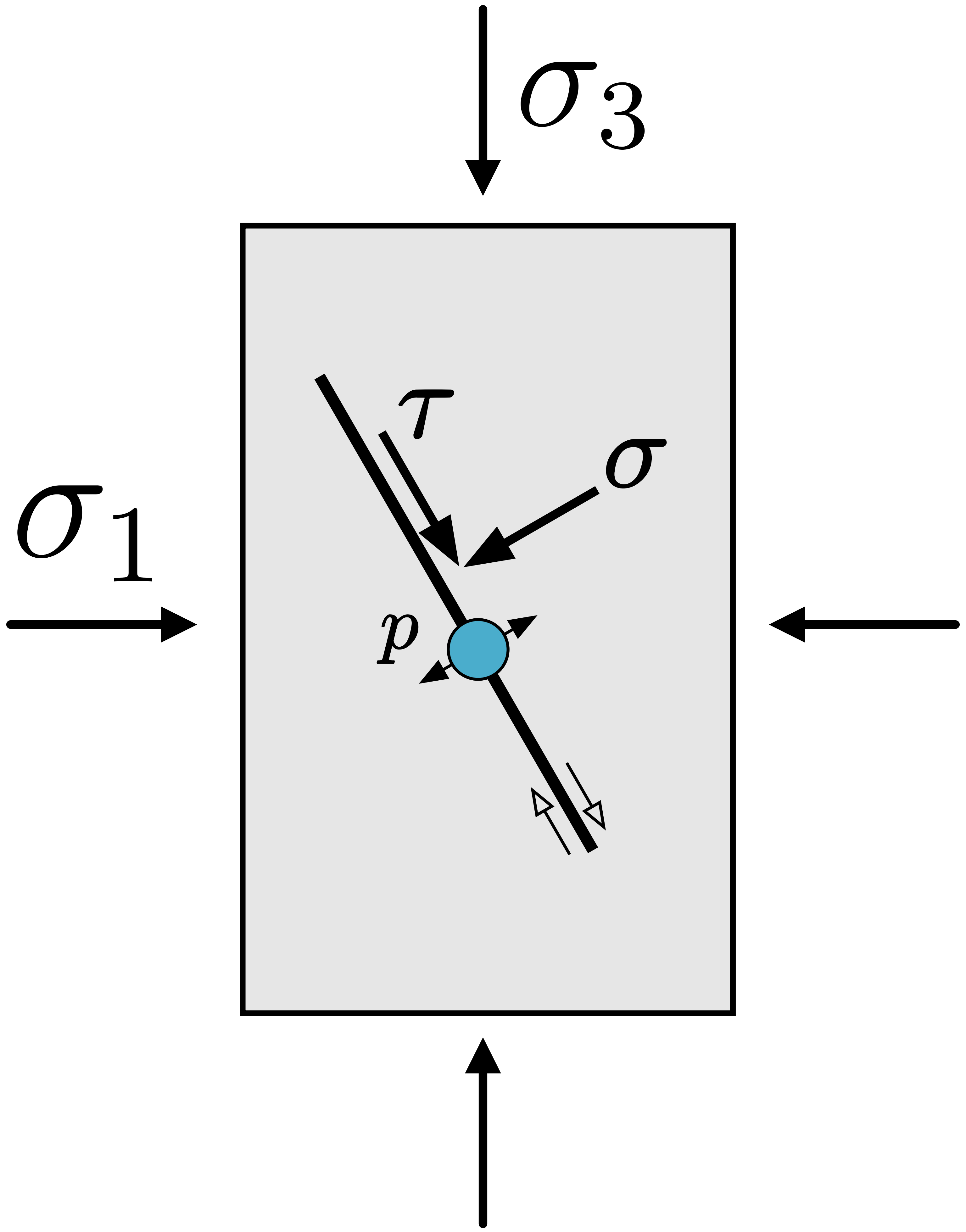

In the case of an isotropic linear elastic porous material the relation between the volumetric strain ε and the isotropic effective stress is of the form

$$\varepsilon = \frac{\Delta V}{V} = -C_m \Delta \sigma' = -C_m \Delta \sigma + C_m \alpha \Delta p$$

where Cm denotes the compressibility of the porous material, the inverse of its compression modulus (Cm = 1/K)

$$\alpha = 1 - C_s / C_m$$

This expression for Biot's coefficient is generally accepted in rock mechanics (Biot & Willis, 1957), and in the mechanics of other porous materials, such as bone or skin (Coussy, 2004). **For soft soils the value of α is close to 1.**

Drained vs. Undrained response

As a way of introducing some basic terminology, consider two idealized experiments. First, imagine an experiment in which a cube of fluid-saturated rock is subject to an isotropic stress. The sample is jacketed with an impermeable membrane that prevents fluid from leaving (or entering) the sample.

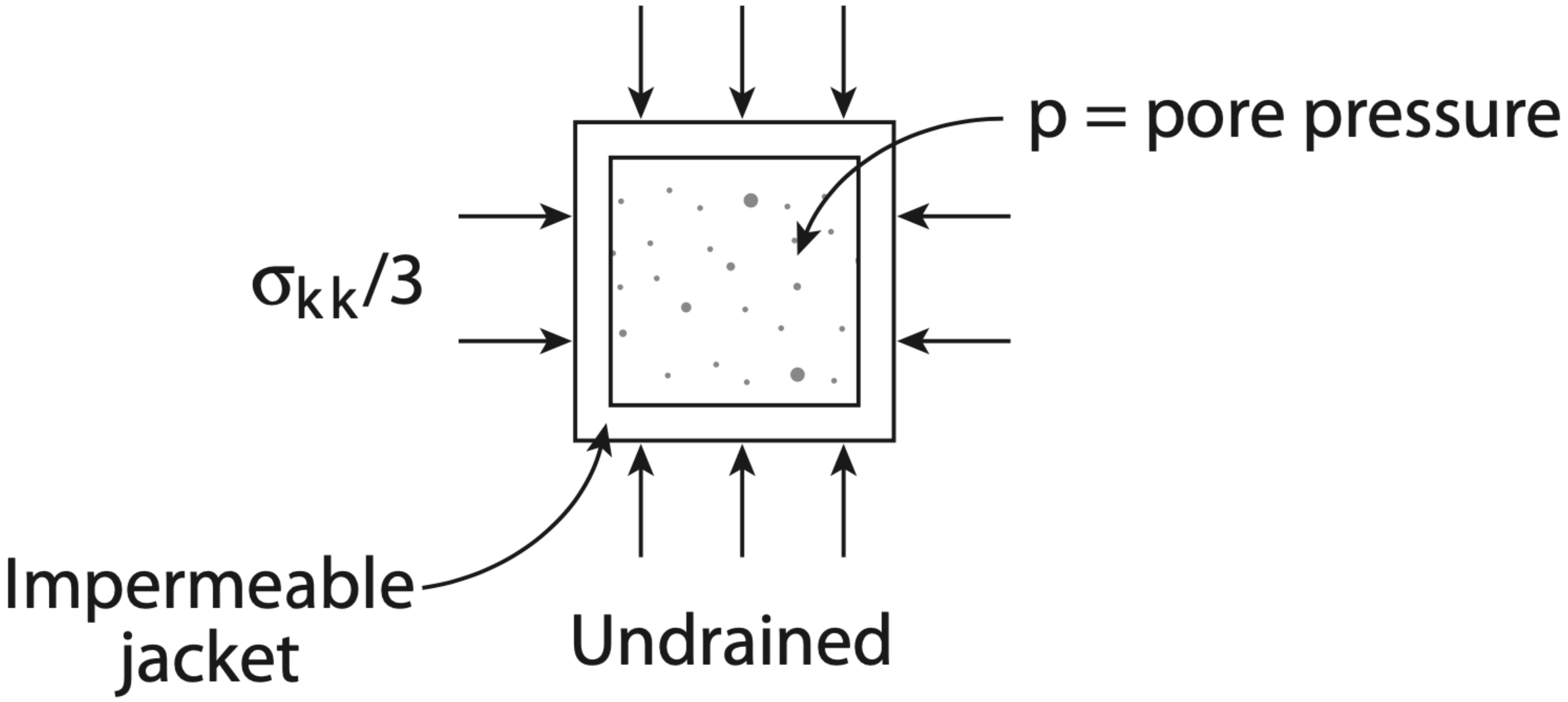

This is referred to as an **undrained test**, since drainage of the fluid is restricted by the impermeable membrane.

Drained vs. Undrained response

One end-member is the **drained test**. In this case, the sample is deformed so slowly that the pore pressures always maintain equilibrium with an external reservoir at constant pressure. Deformation at long times after the application of a load approaches a fully drained state.

This is an excellent analogy with viscoelasticity:
The undrained poroelastic response corresponds to the unrelaxed viscoelastic response, while the drained poroelastic response corresponds to the fully relaxed viscoelastic response.

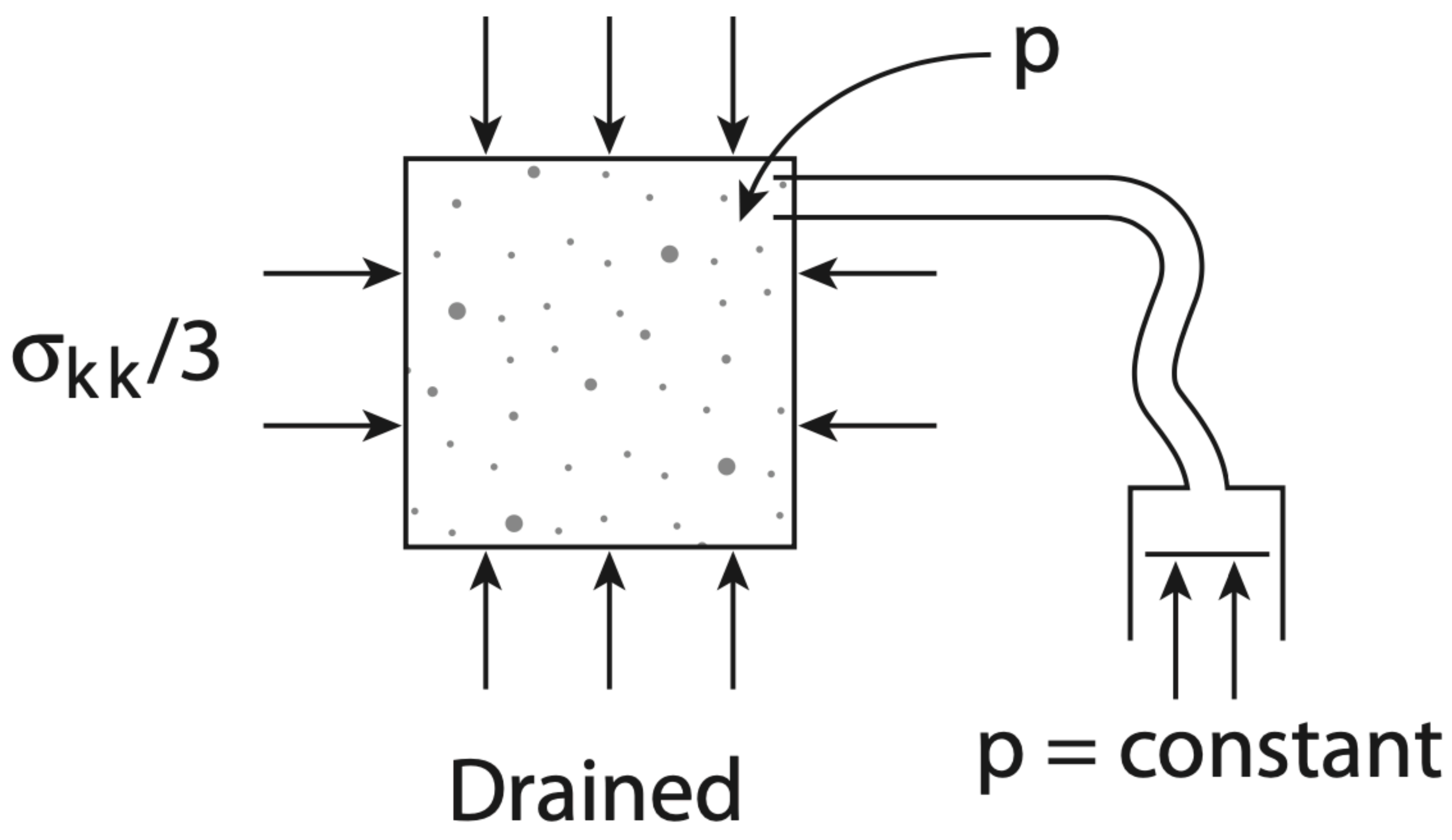

If the sample is deformed very rapidly, the deformation can be effectively undrained, even without the impermeable membrane. If the deformation is imposed rapidly, and one considers only short times before fluid flow has had a chance to occur, the deformation is effectively undrained.

Drained vs. Undrained response

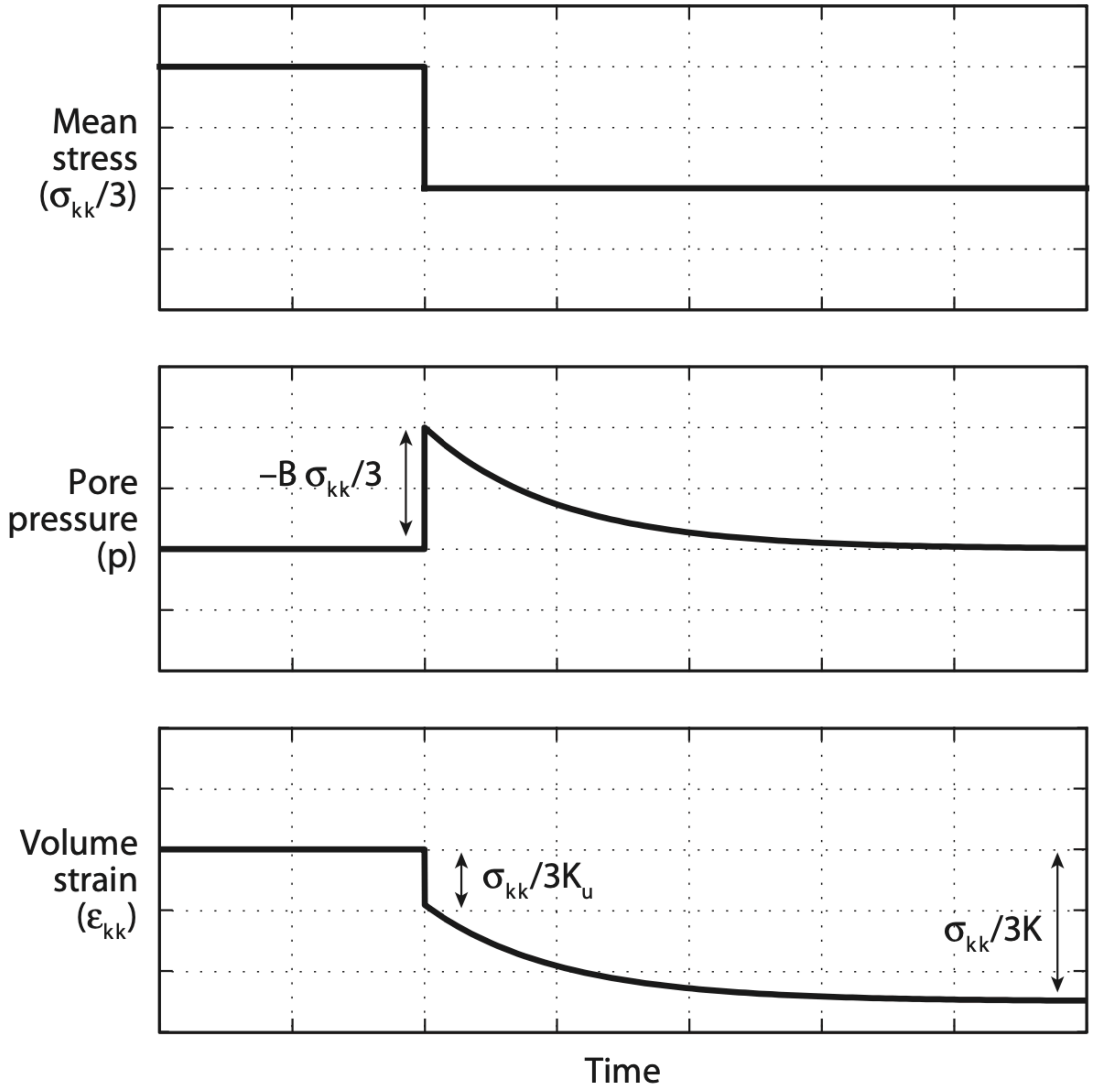

Consider an idealized experiment in which a cube of porous rock is subjected to a step change in confining stress, $-\Delta\sigma_{kk}/3$

Simultaneously, the pore pressure increases by an amount:

$$p = -B\Delta\sigma_{kk}/3$$

The applied compression causes the rock to contract instantaneously by an amount $-\Delta\sigma_{kk}/3\ K_u$ where K_u is the undrained bulk modulus.

As fluid flows out, the rock becomes more compliant, and the volumetric strain gradually approaches $-\sigma_{kk}/3\ K$, where K is the ordinary, or drained bulk modulus.

Pore-fluid pressure effects on faults

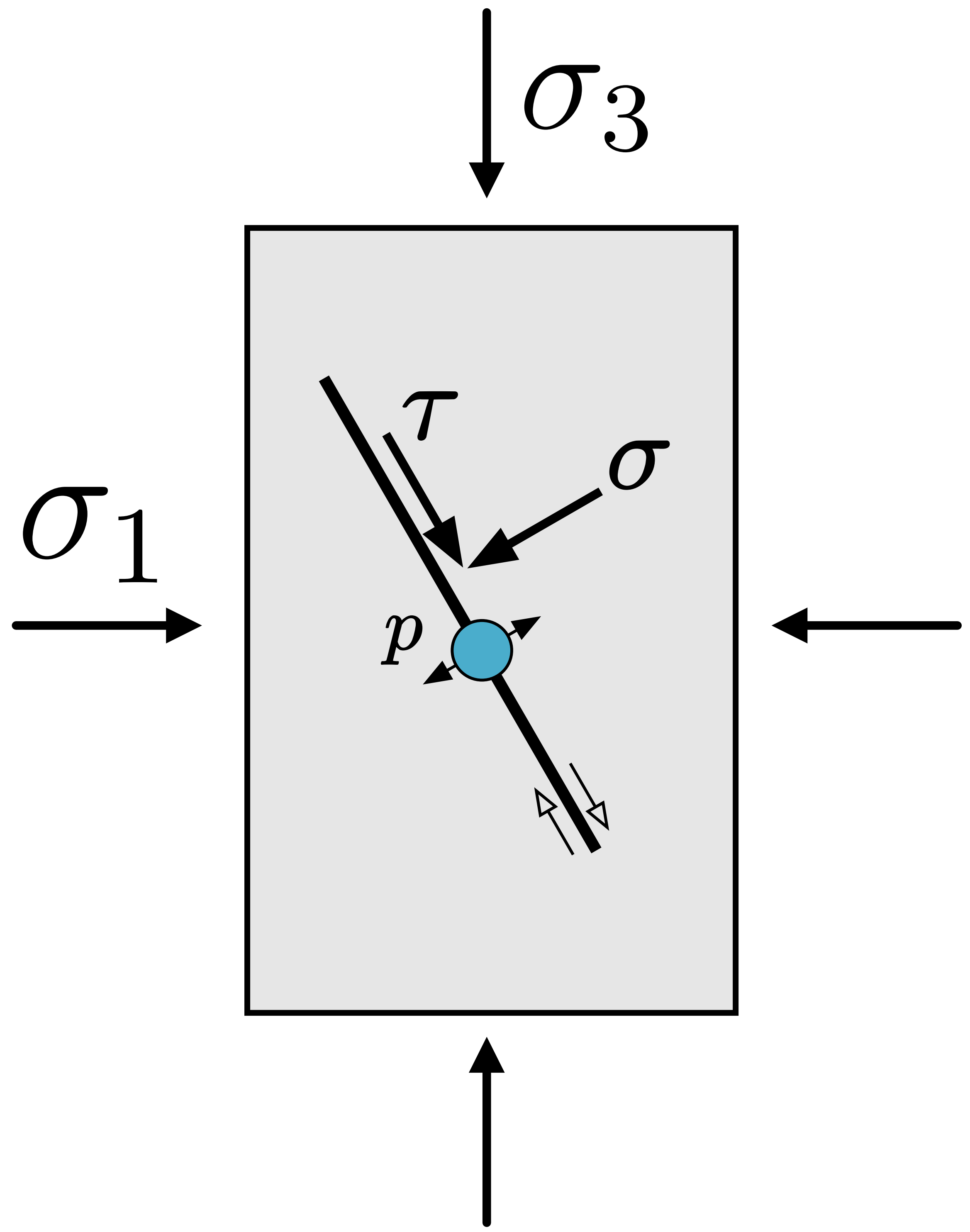

Effective normal stress

$$\tau = f\,(\sigma - p)$$

Shear stress

Friction (Rate-and-state)

Normal stress

Pore pressure

Pore-fluid pressure effects on faults

Effective normal stress

$$\tau = f\,(\sigma - p)$$

Shear stress

Friction
(Rate-and-state)

Normal stress

Pore pressure

1. **Direct injection-induced variations in pore pressure**
2. **Shear dilatancy/compaction-induced variations in pore pressure**
3. **Variation in pore pressure due to poroelastic bulk**

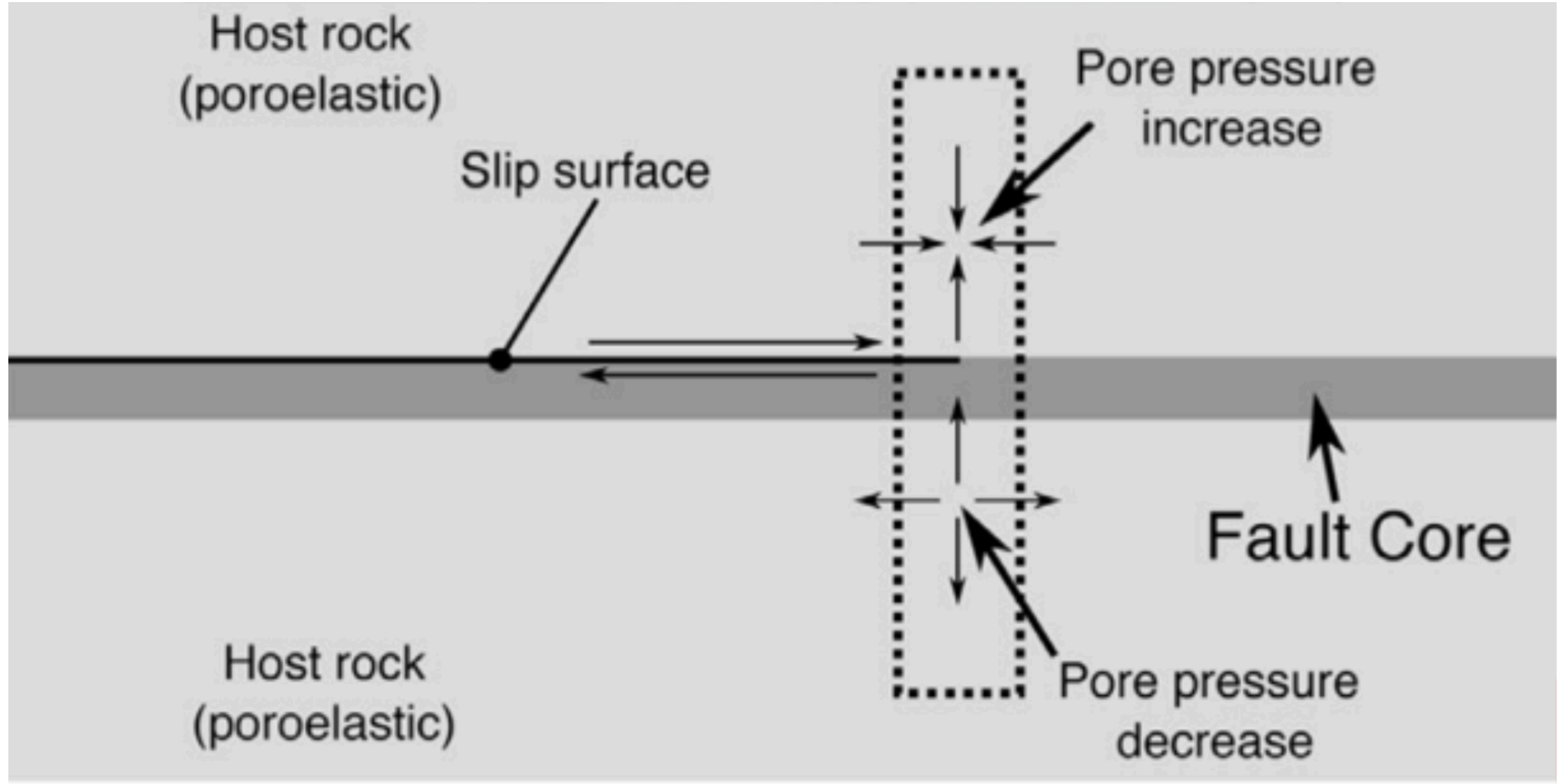

Field experiment on fluid injection: aseismic and seismic slip

The fault is instrumented with seismometers and a fiber-optics probe that measures fault displacement and fluid pressure

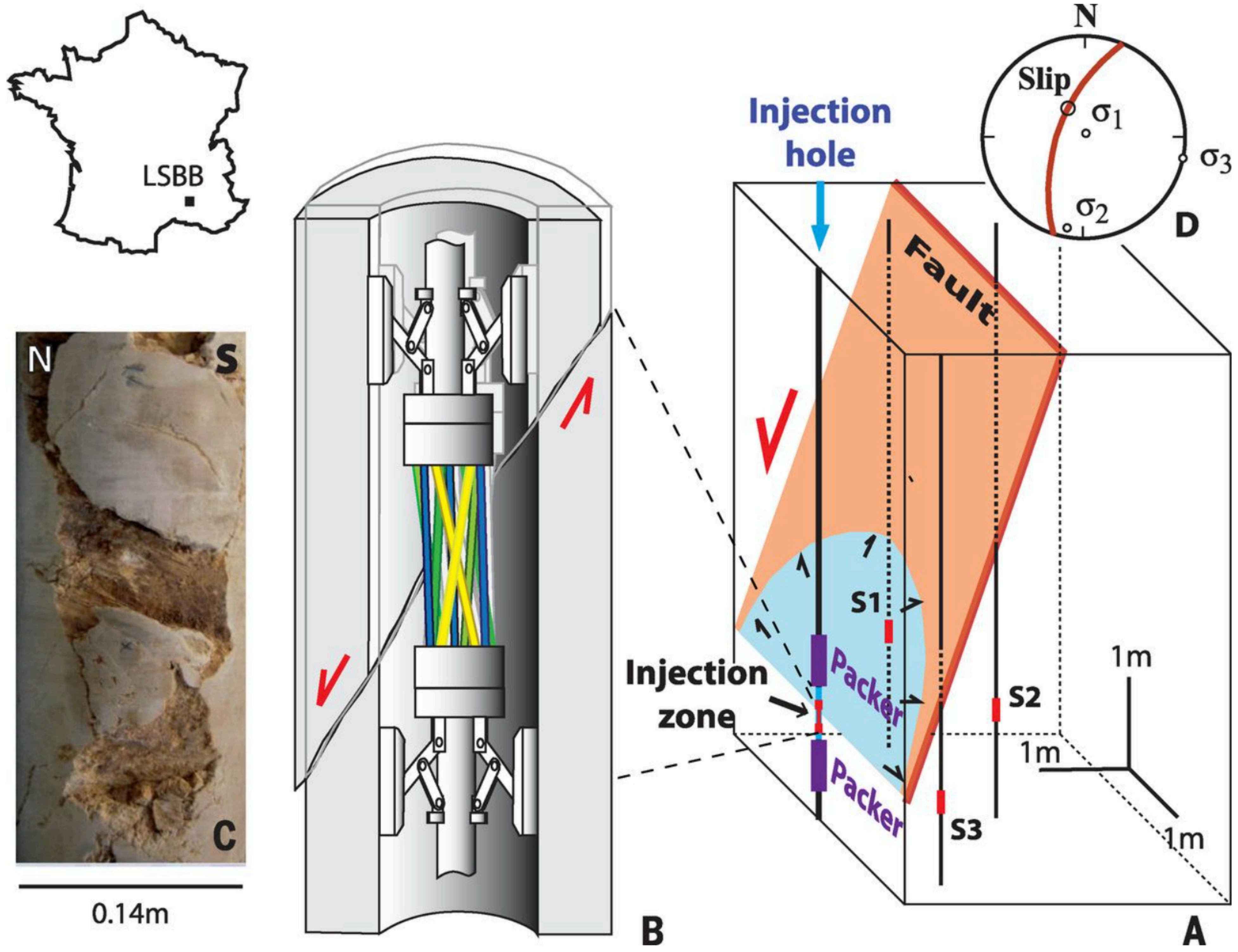

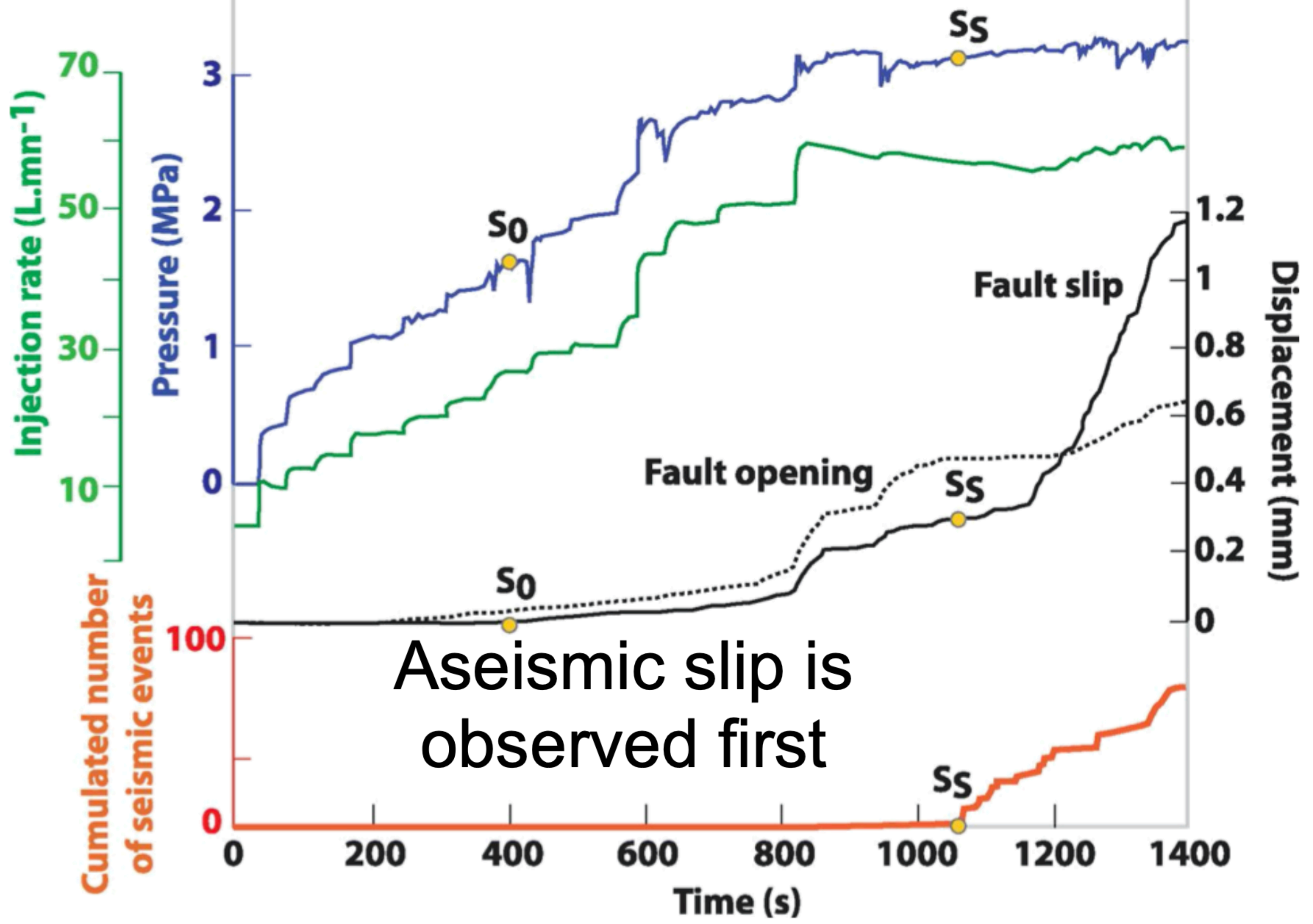

Guglielmi, Cappa, Avouac et al., (2015)

Field experiment on fluid injection: aseismic and seismic slip

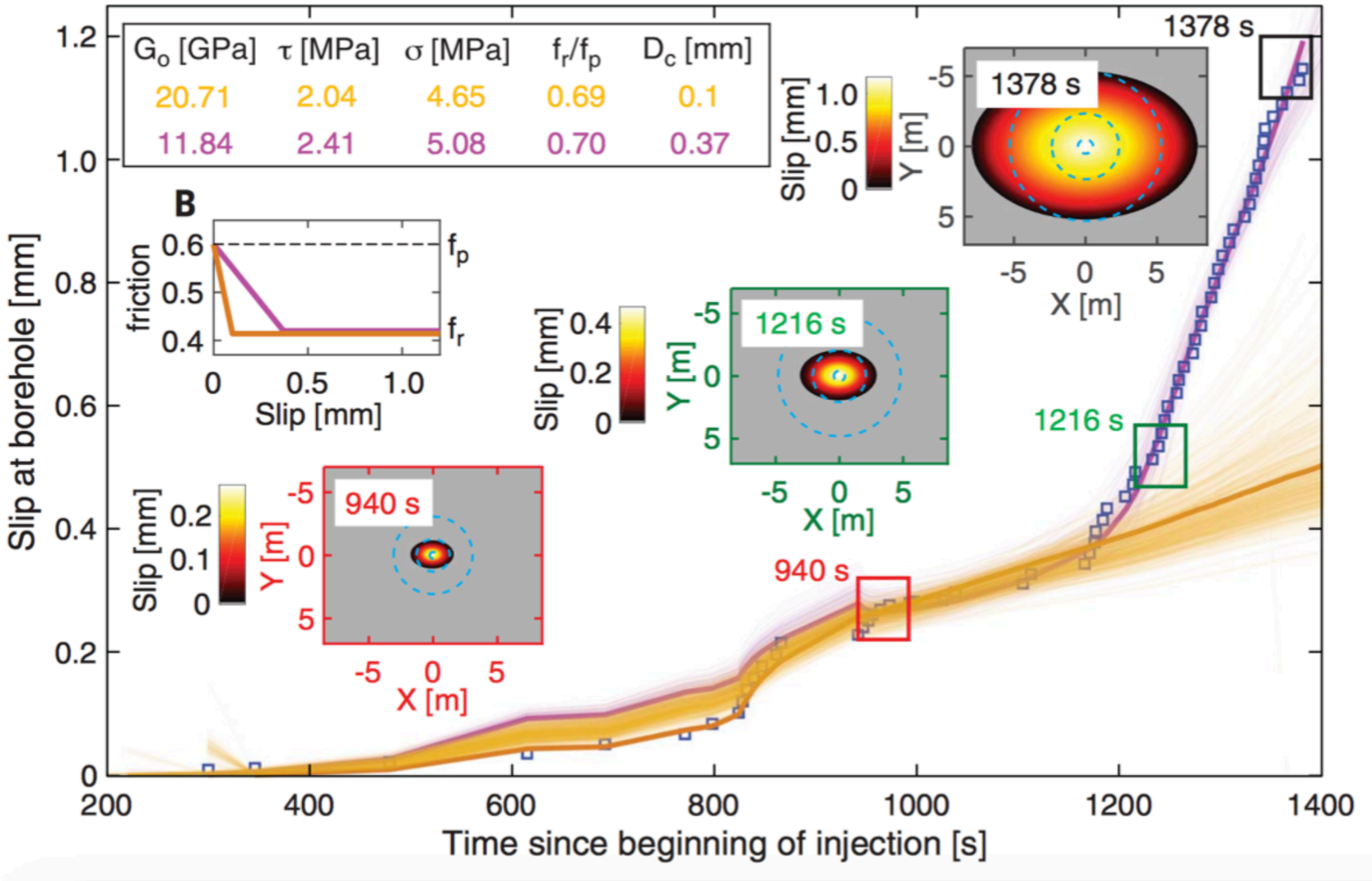

Study with slip-weakening friction:
Fault slip outpaces fluid migration

Bhattacharya and Viesca, 2019

Fluid injection into rate-and-state fault

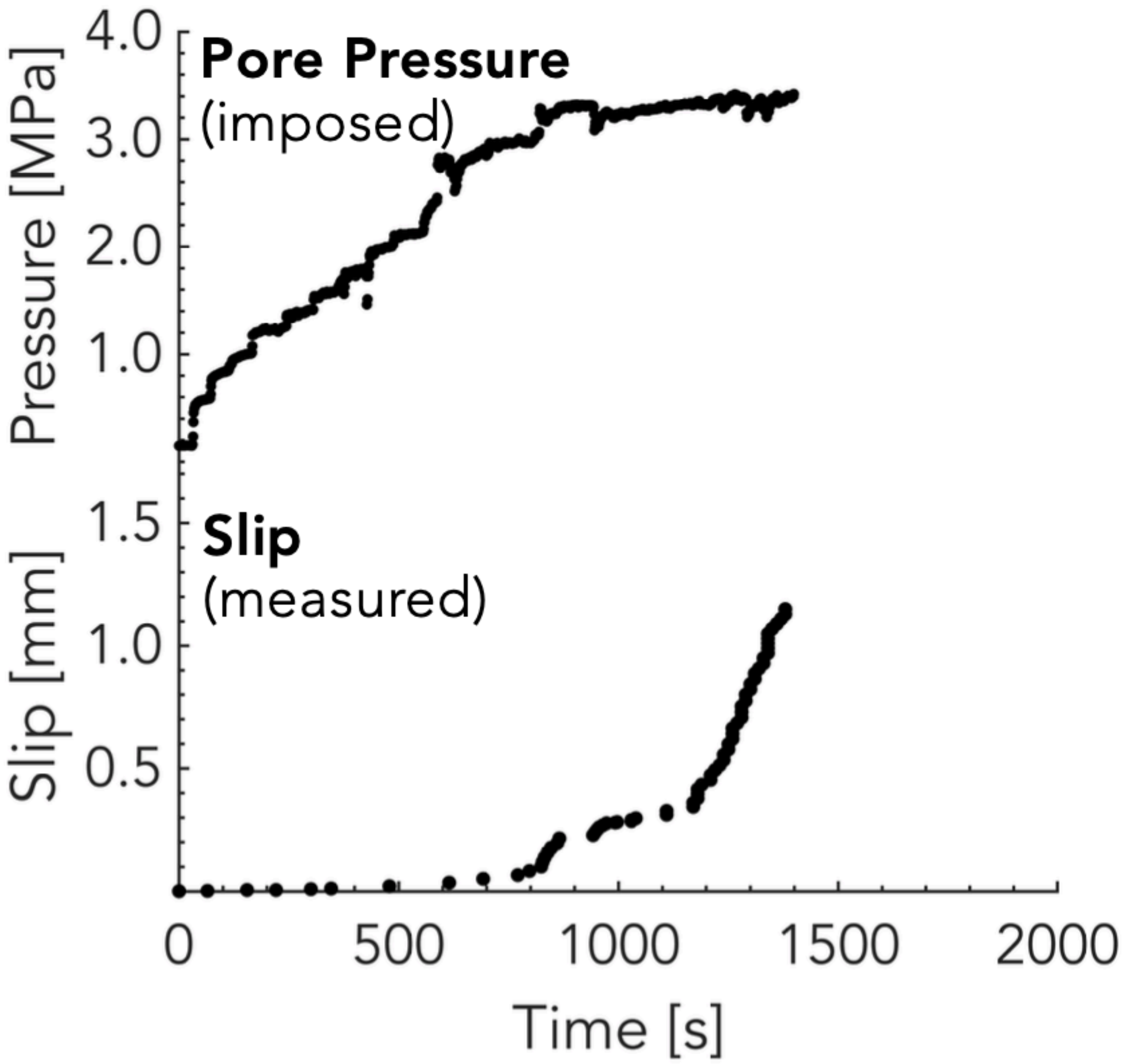

Multiple scenarios can explain the fault slip observed during the field experiment

Fluid injection into rate-and-state fault

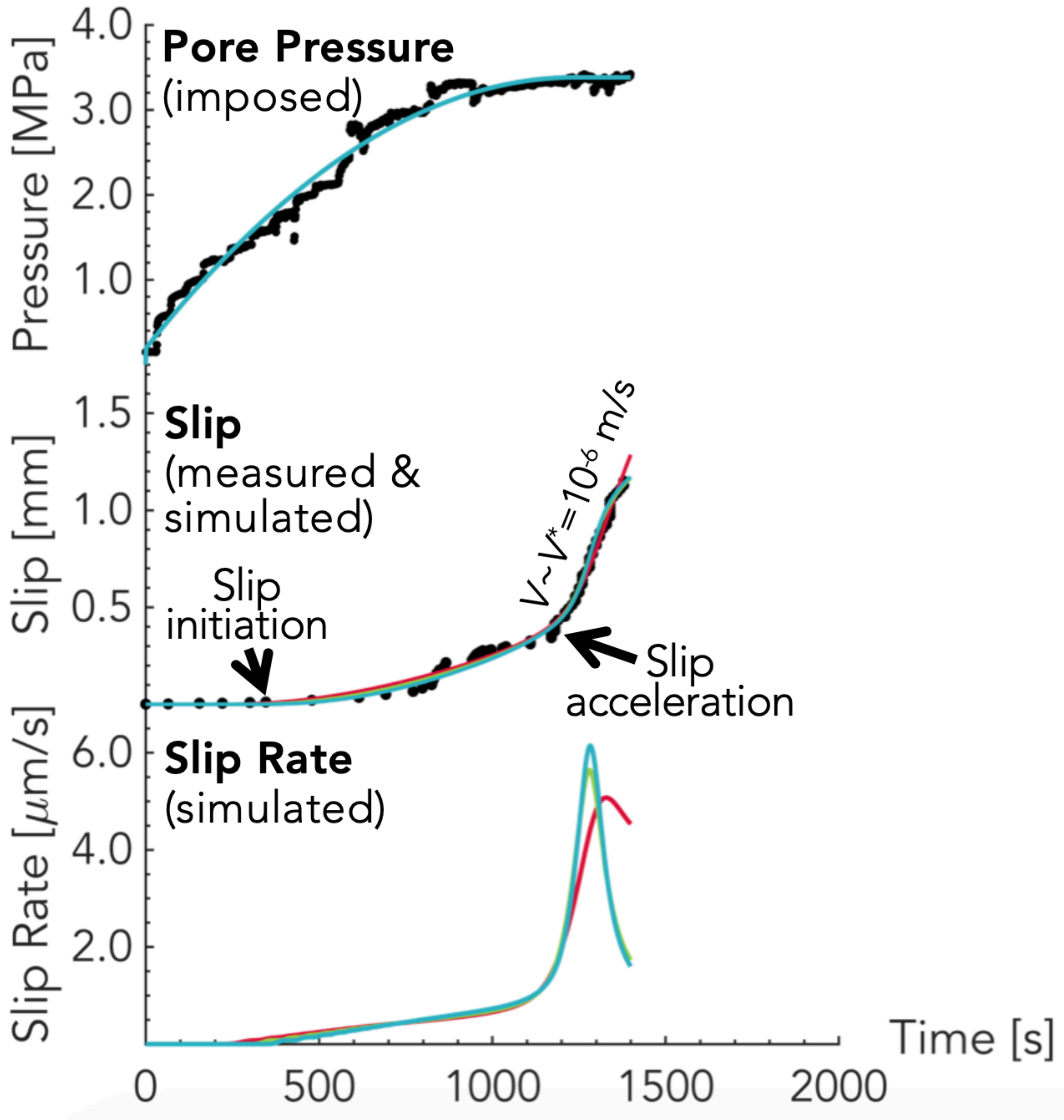

Properties	Lower Friction	Intermediate Friction	Higher Friction
f_{ini}	0.54	0.54	0.54
f^*	**0.48**	**0.55**	**0.60**
a-b	-0.001	-0.005	0.005
b	0.016	0.016	0.016
L [μm]	16.75	16.75	16.75
α [m²/s]	**0.04**	**0.20**	**0.85**
μ [GPa]	10	10	10
θ_{ini} [s]	1.2e12	2.4e12	7.0e12

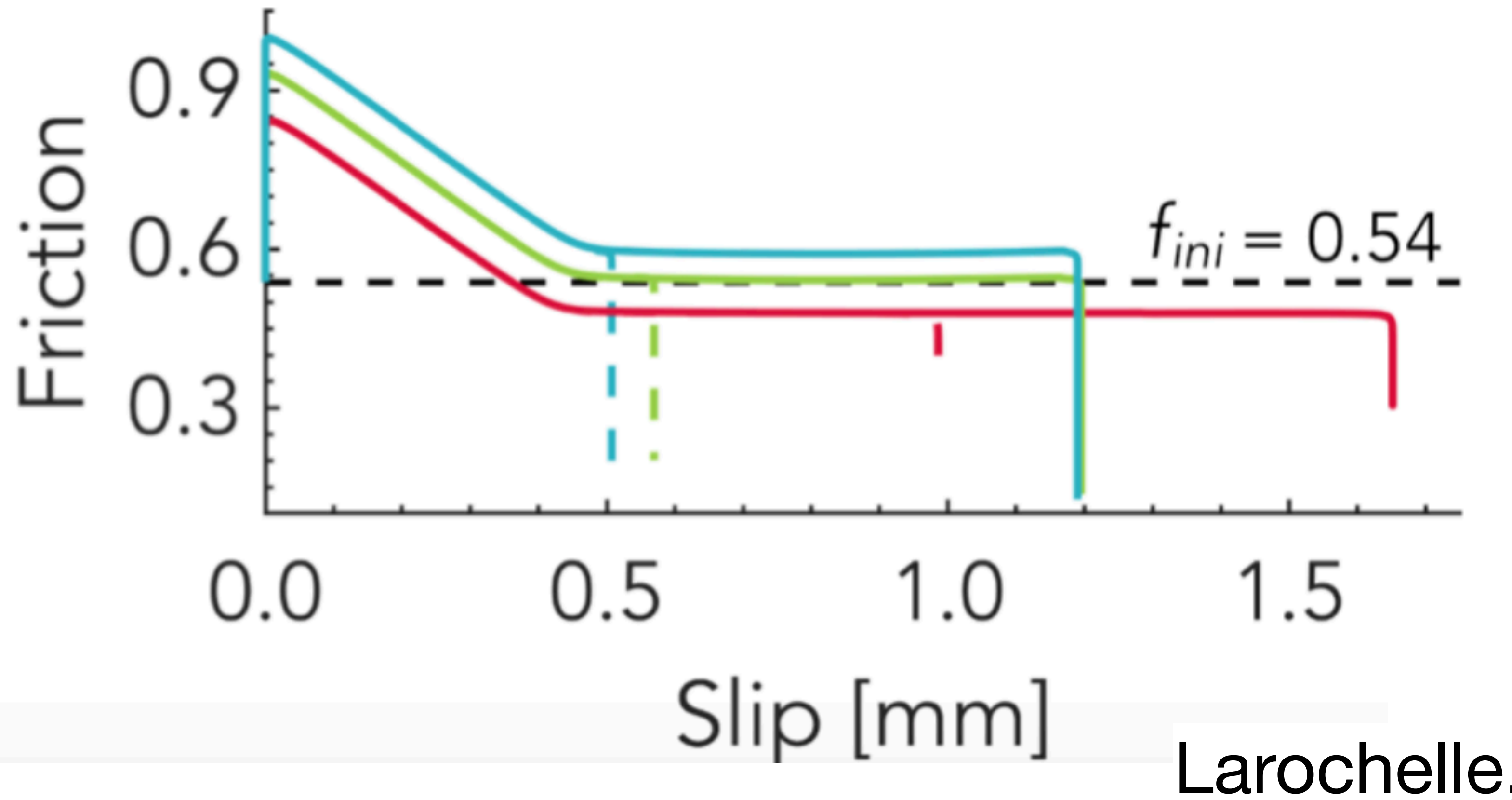

Larochelle, Lapusta et al. (2021)

Fluid injection into rate-and-state fault

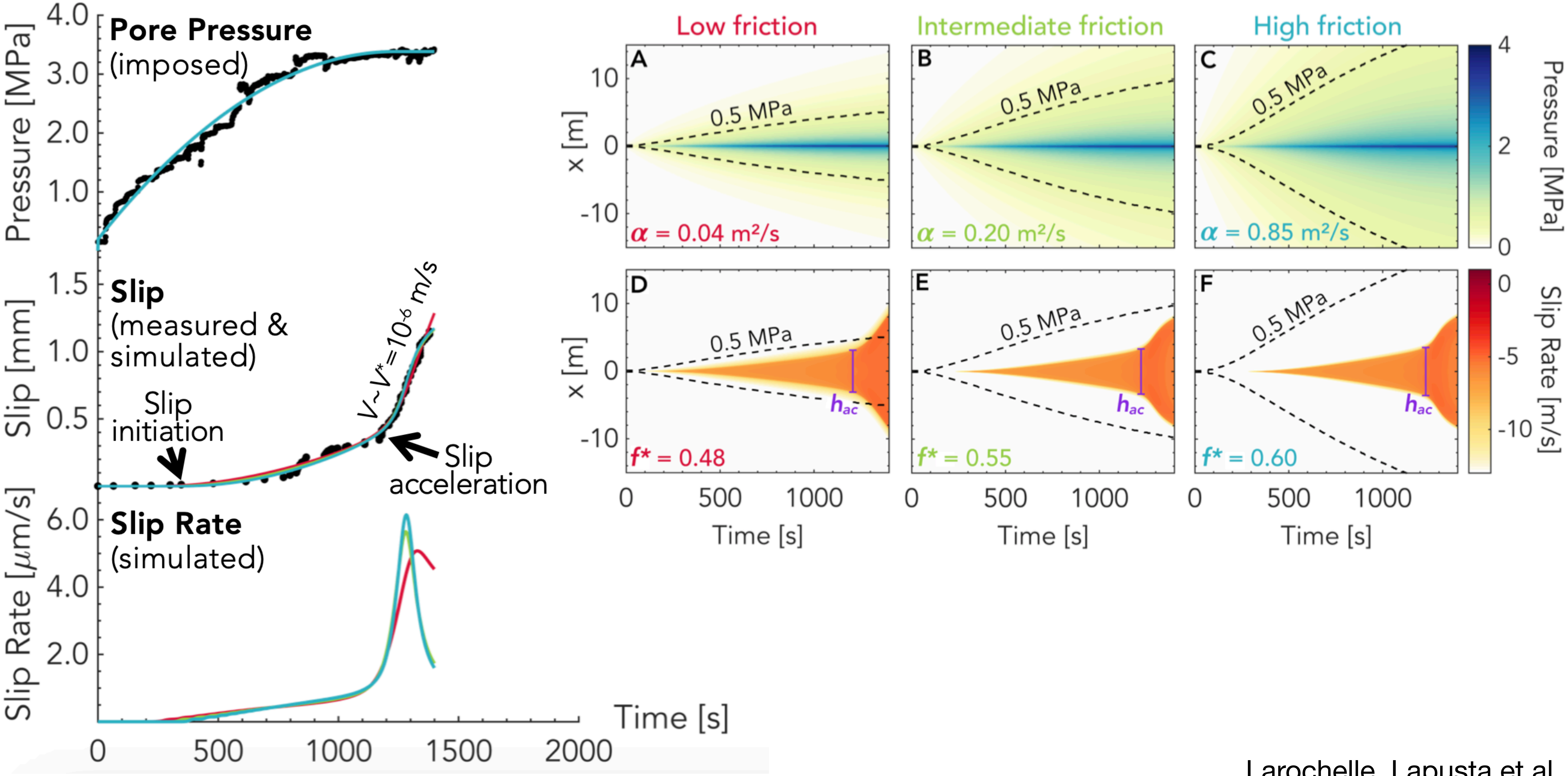

Larochelle, Lapusta et al. (2021)

Fluid injection into rate-and-state fault

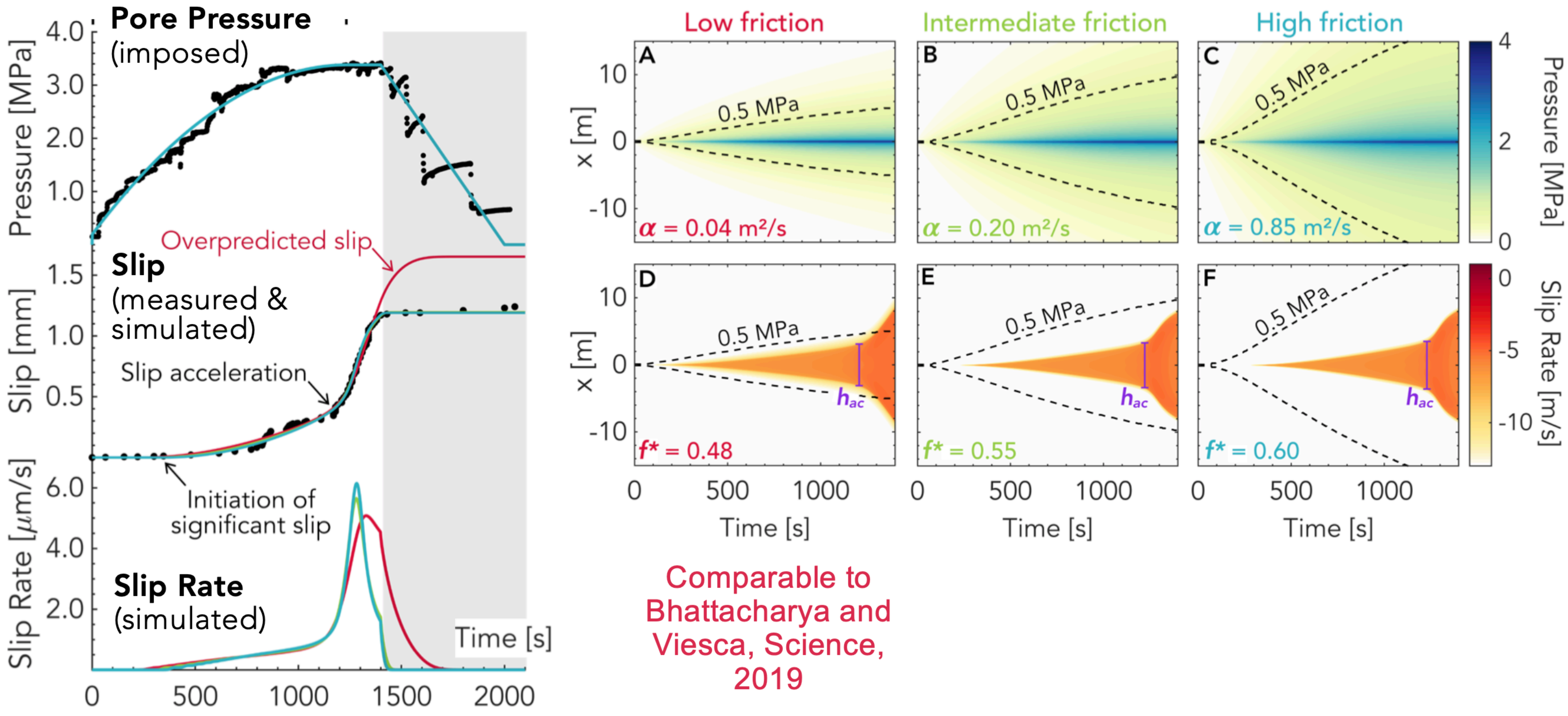

Comparable to Bhattacharya and Viesca, Science, 2019

Larochelle, Lapusta et al. (2021)

Fault stability during fluid injection experiments

Bedretto Underground Laboratory for Geosciences & Geoenergies

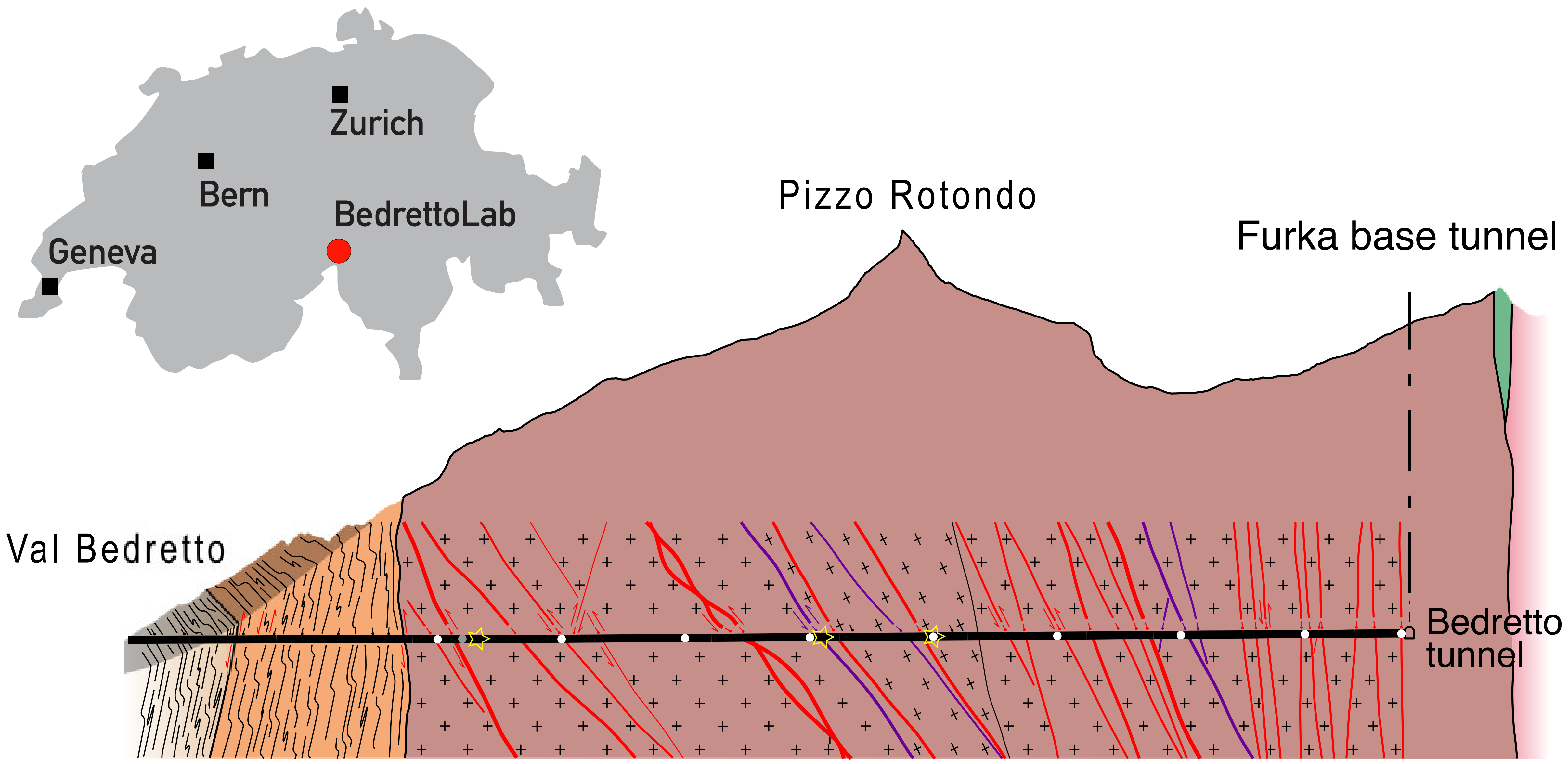

Schweizerischer Erdbebendienst
Service Sismologique Suisse
Servizio Sismico Svizzero
Swiss Seismological Service

ETH zürich

INGV

RWTH
RHEINISCH-WESTFÄLISCHE TECHNISCHE HOCHSCHULE AACHEN

SAPIENZA
UNIVERSITÀ DI ROMA

Fault stability during fluid injection experiments

Bedretto Underground Laboratory for Geosciences & Geoenergies

FEAR project

("Fault Reactivation and Earthquake Rupture")

- With the European project FEAR we are conducting a suite of **injection experiments** in the Bedretto Underground Laboratory (BedrettoLab).

- The goal of FEAR is to gain understanding on how earthquakes start and stop by using hydraulic stimulation to initiate small earthquakes (magnitude ~1 events on a fault of ~50m scale).

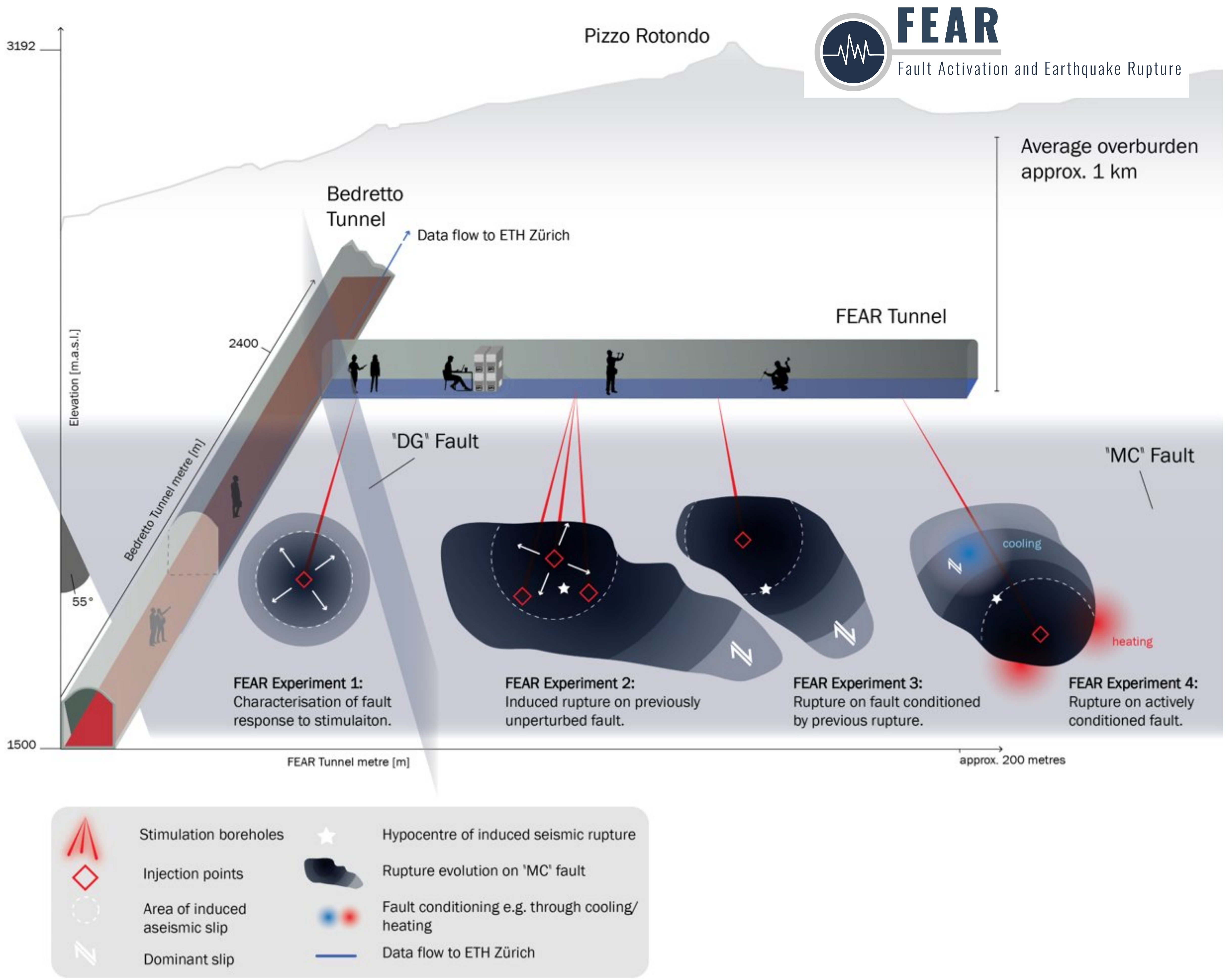

erc
European Research Council

Fault stability during fluid injection experiments

Laboratory experiments on fault gouge indicate that the frictional properties of some faults are slightly velocity-strengthening (a-b>0)

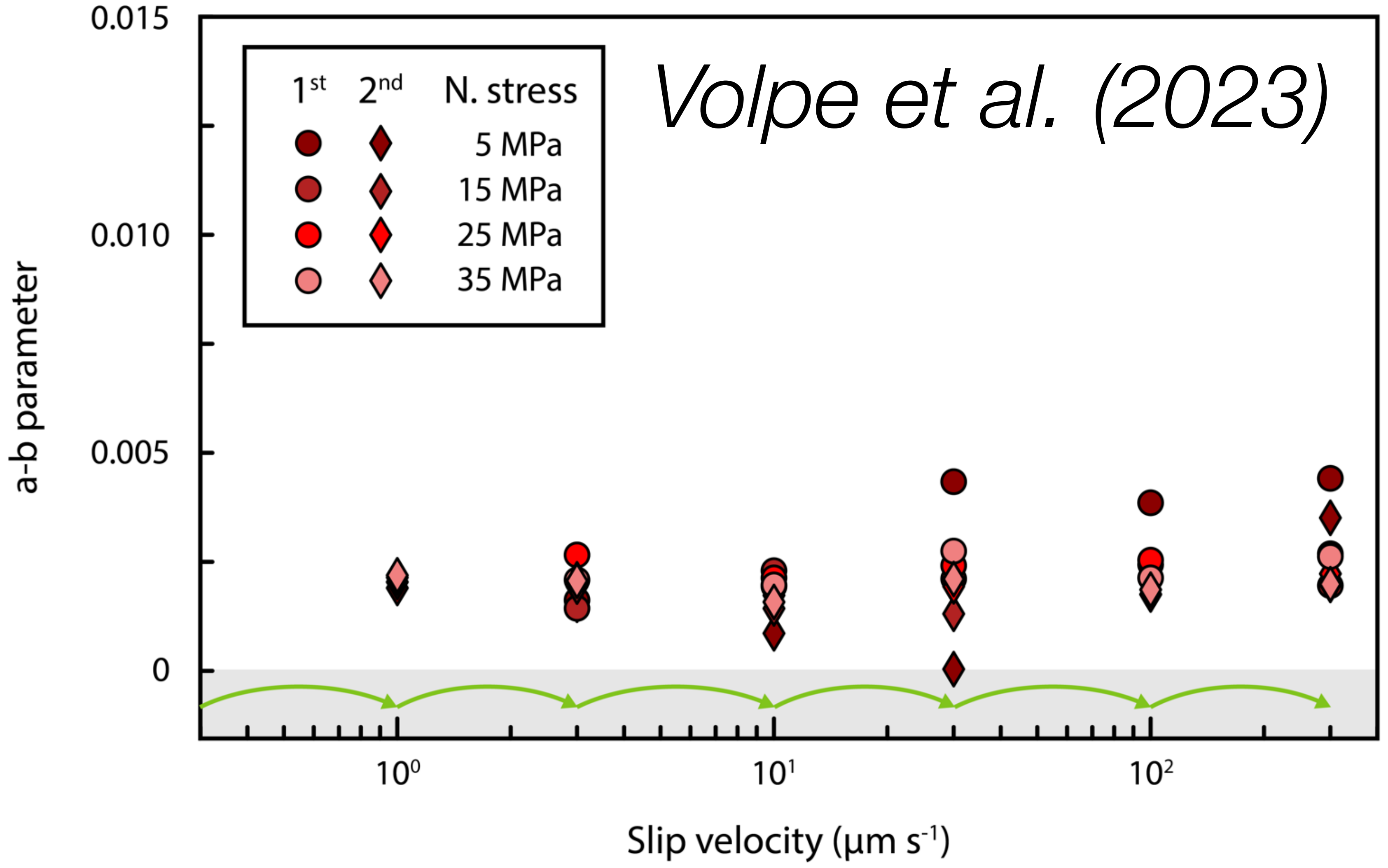

Tectonic faults are often assumed to slip either slow due to stable, velocity-strengthening frictional behavior, or fast as a result of velocity-weakening friction leading to dynamic (seismic) rupture.

As a consequence, velocity-strengthening faults may be regarded as intrinsically stable as they do not spontaneously nucleate seismic events.

Fault stability during fluid injection experiments

Laboratory experiments on fault gouge indicate that the frictional properties of some faults are slightly velocity-strengthening (a-b>0)

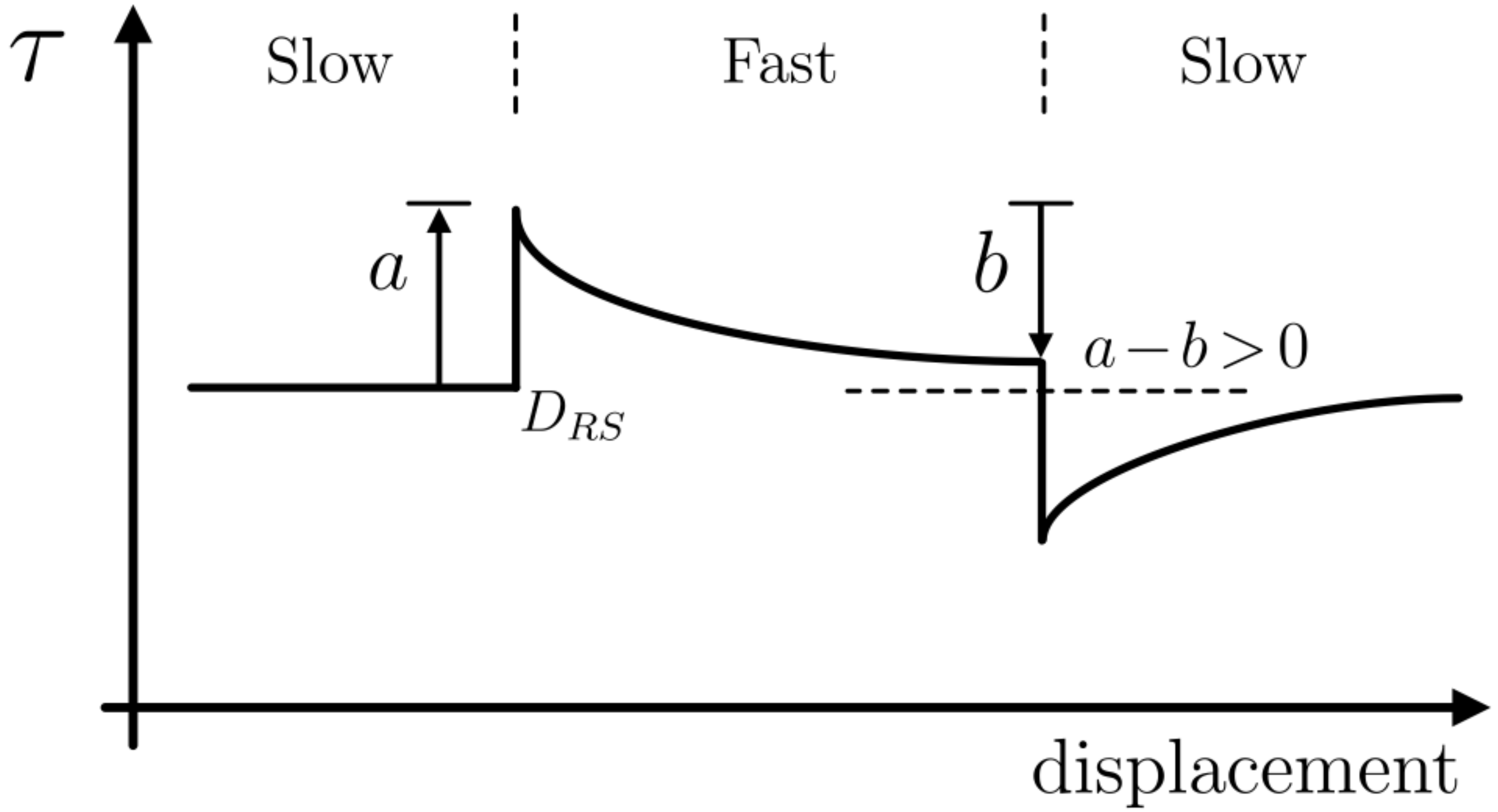

Can seismic ruptures nucleate on nominally stable velocity-strengthening faults?

Fault stability during fluid injection experiments

To tackle this problem, we developed the first **H**ydro-**M**echanical **E**arthquake **C**ycle**s** code (H-MECs) to simulate fault slip in a fully coupled and compressible poro-visco-elasto-plastic medium.

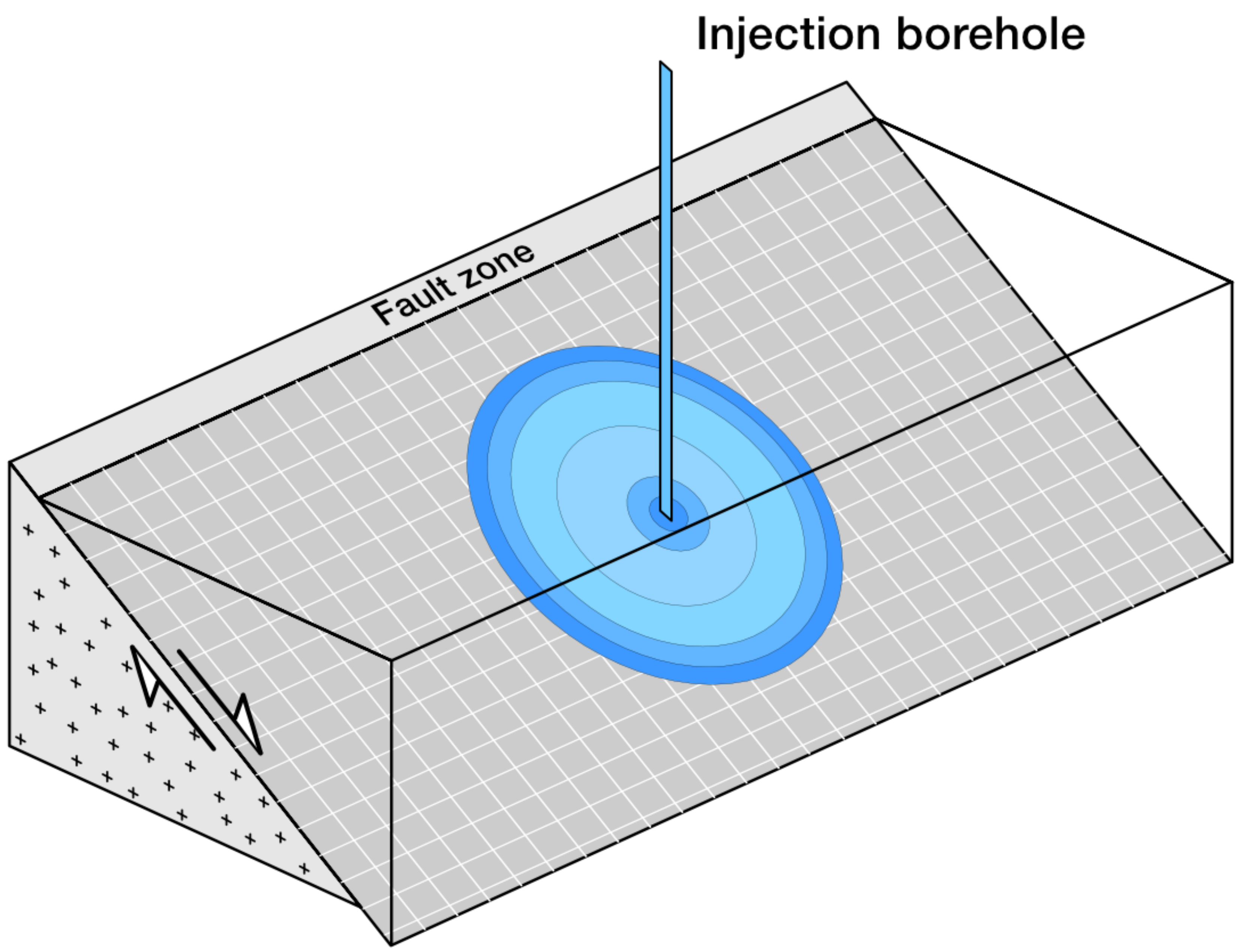

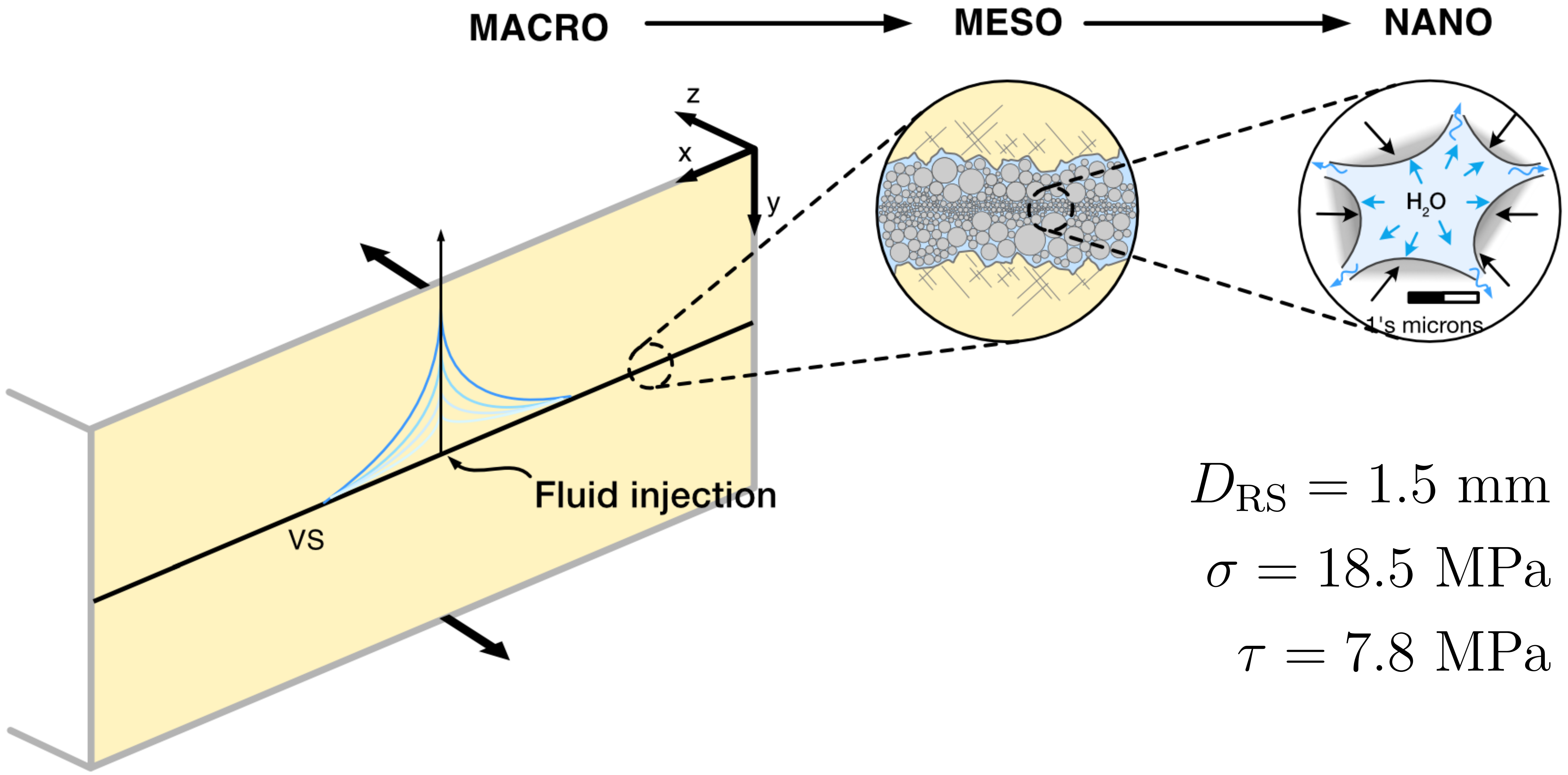

$$D_{\mathrm{RS}} = 1.5 \text{ mm}$$
$$\sigma = 18.5 \text{ MPa}$$
$$\tau = 7.8 \text{ MPa}$$

We designed ad-hoc numerical model by exploiting the exploiting the constraints and data provided by the BedrettoLab.

Fault stability during fluid injection experiments

Based on the constitutive relationships of linear poroelasticity (*Wang, 2000*), we vary the fault gouge compressibility inside the fault zone to explore a broad range of both Biot and Skempton's coefficients

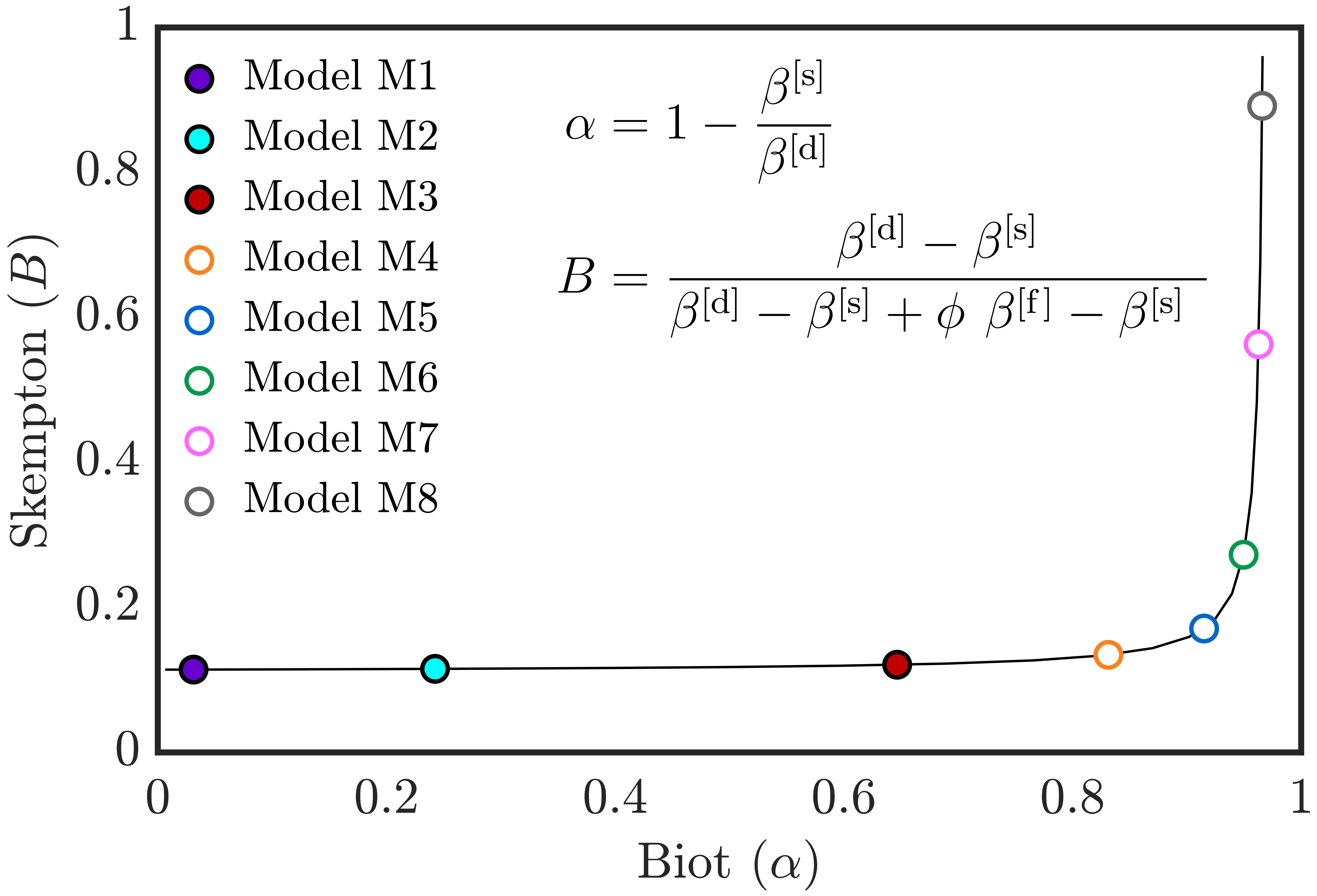

Biot: 0-to-1 dimensionless parameter to describe the mechanical interaction between a porous medium and the fluid contained within its pores. Values near 1 indicating that the fluid pressure significantly impacts the effective stress.

Skempton: 0-to-1 dimensionless parameter that quantifies how much of the applied stress is transferred to the pore water pressure and thus influences the deformation and strength properties of the porous material.

$\beta^{[f]}$ **Fluid compressibility** (water): $4 \cdot 10^{-10}$ 1/Pa

$\beta^{[s]}$ **Fault gouge compressibility?** We don't know!

~$1–4 \cdot 10^{-11}$ 1/Pa

Fault stability during fluid injection experiments

The response of the fault to fluid injection (0.5 MPa/min) is characterized by short periods of fluid pressurization from the injection point where the fault remains locked.

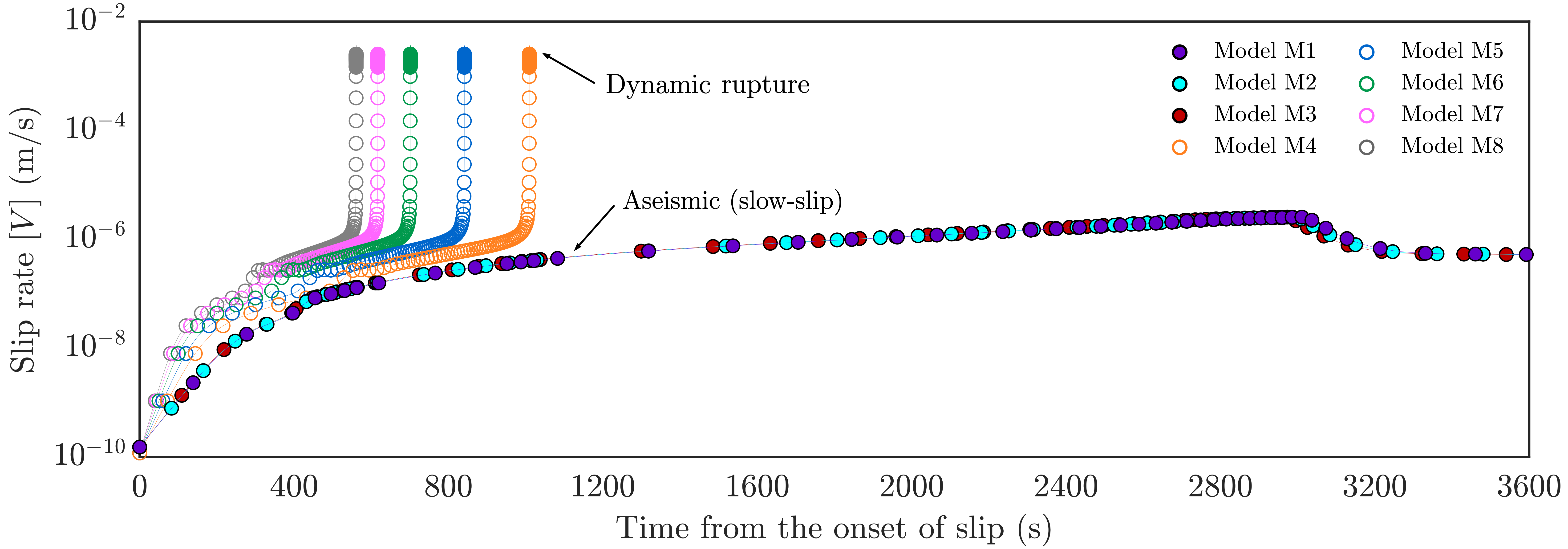

For relatively low values of Biot coefficient (M1–M3), a slow-slip event slightly accelerates over time, but the velocity-strengthening properties on the fault prevents slip instabilities. For high values of Biot and Skempton coefficients (M4–M8), a slow-slip transient promotes a transition to a fast (seismic) event.

Dal Zilio and the BedrettoLab Working Group (2023, in prep.)

Fault stability during fluid injection experiments

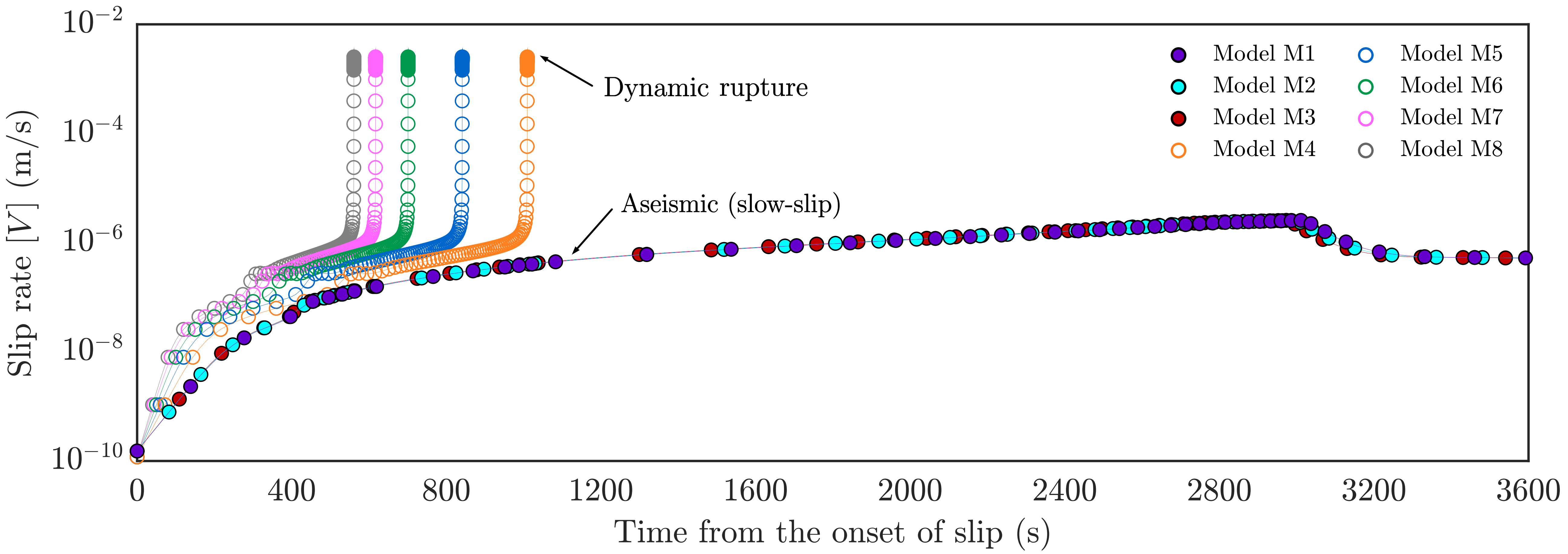

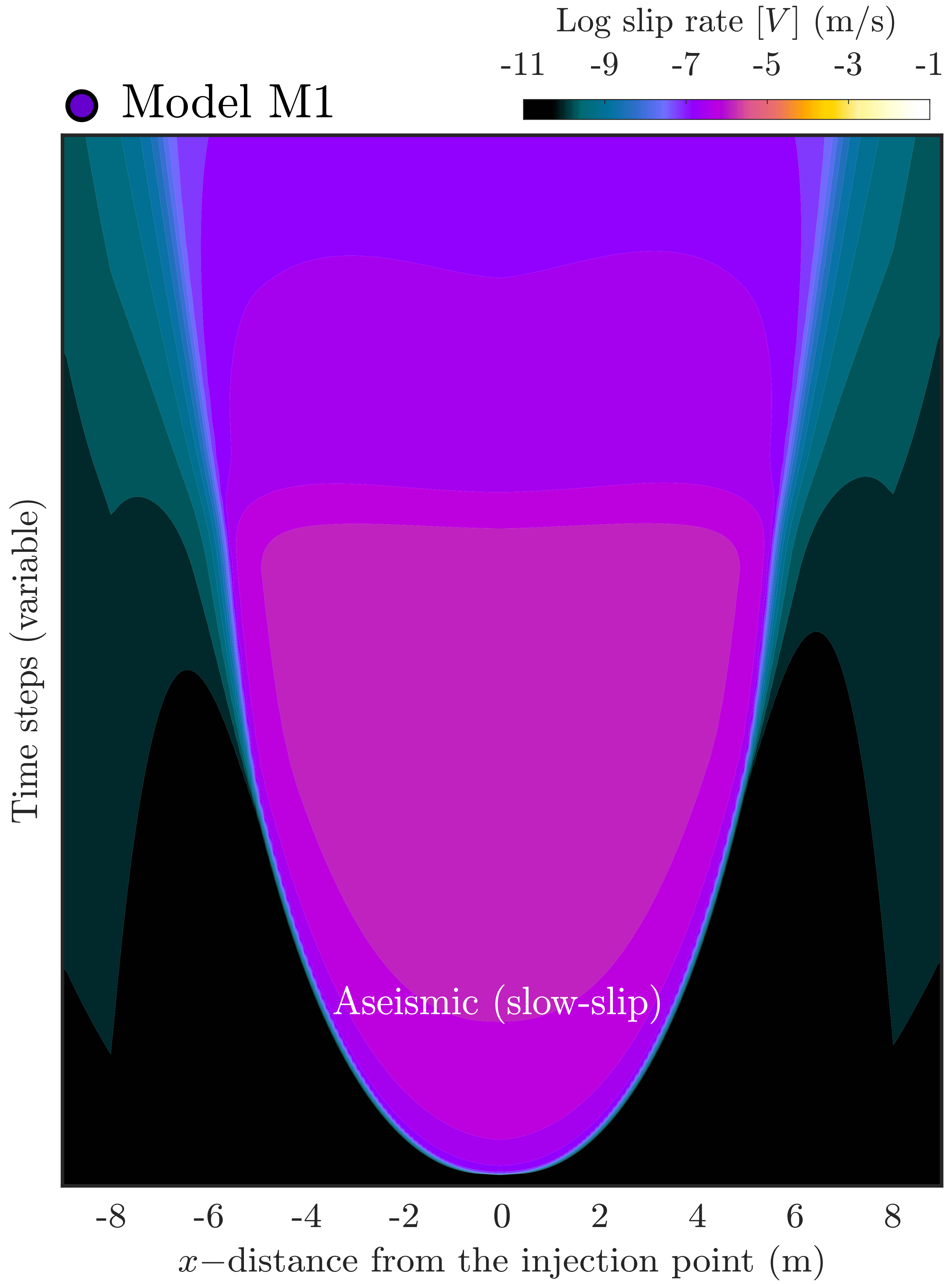

In all experiments, aseismic slip initiates near the location of injection point.

Model M1–M3: Slow-slip events propagate steadily throughout the entire fault segment at rupture speeds of ~km/day

Fault stability during fluid injection experiments

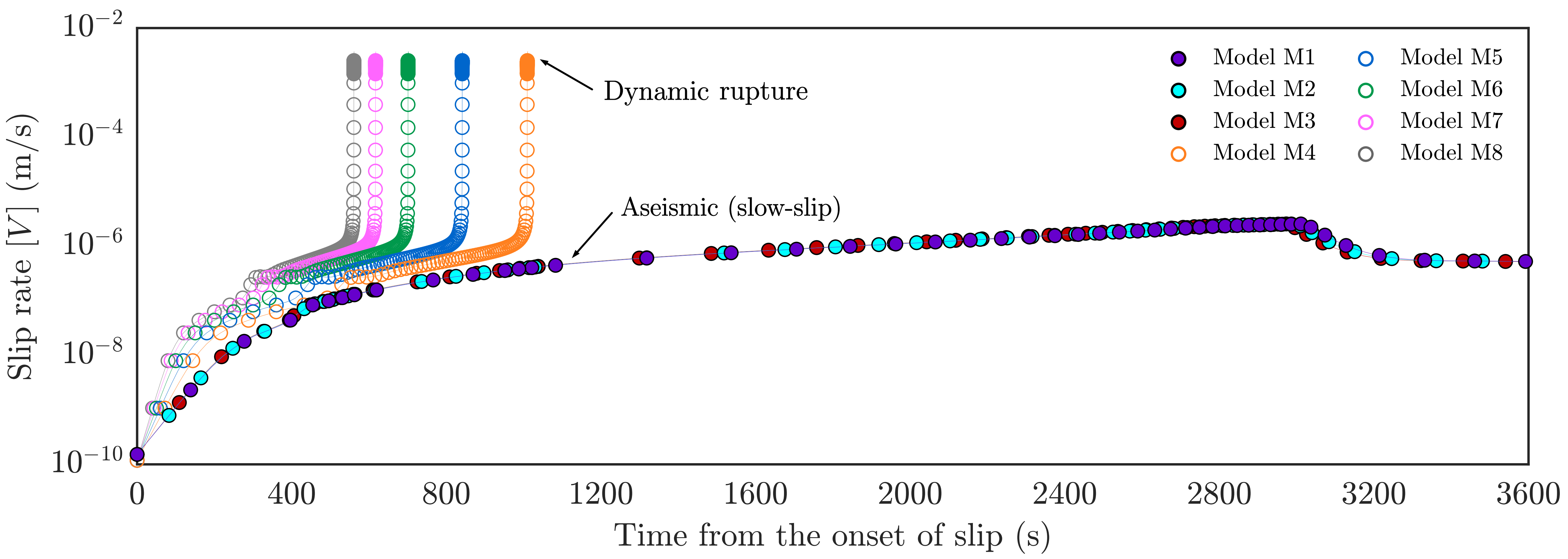

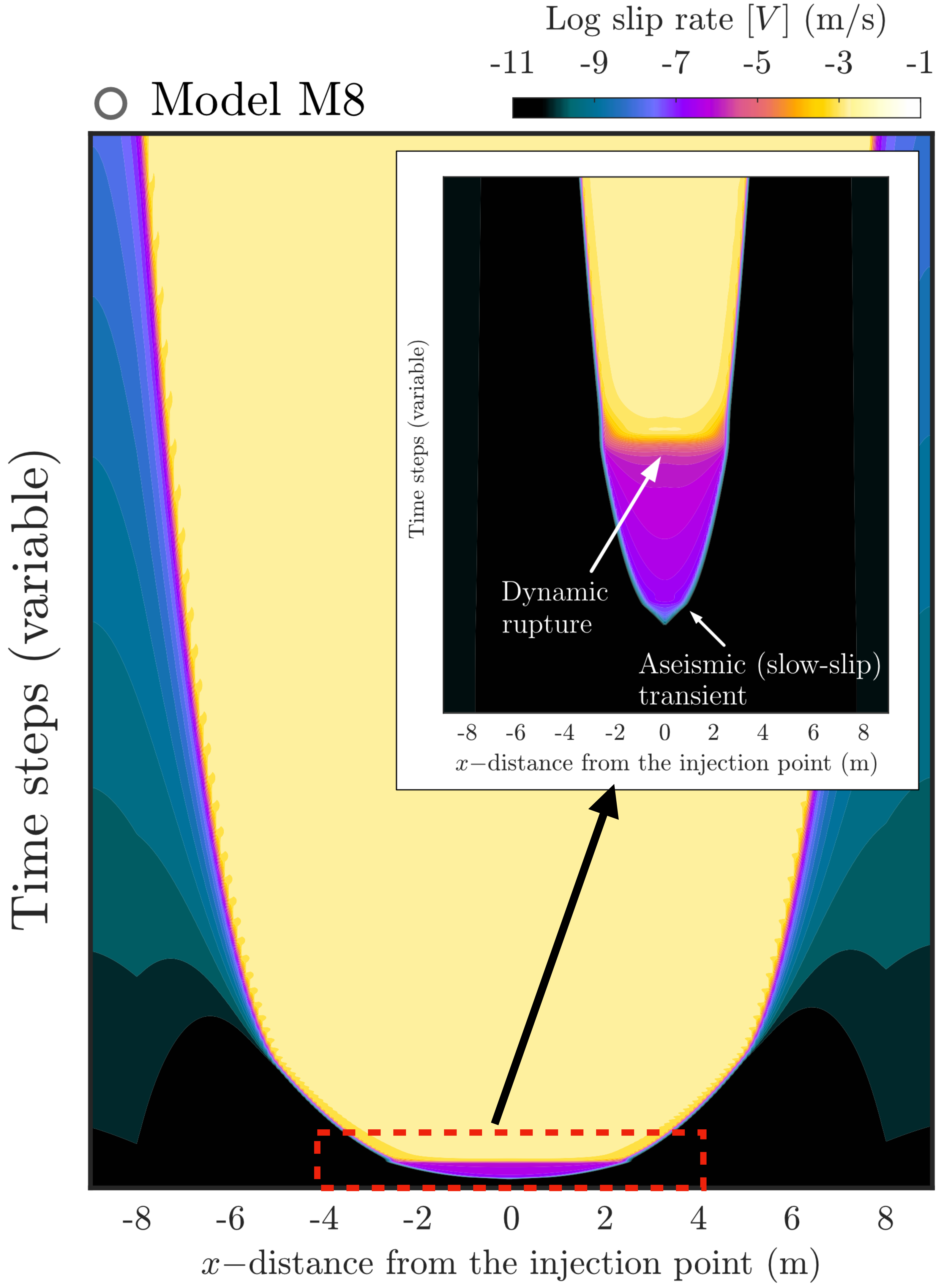

Model M4–M8: Dynamic rupture is preceded by aseismic slip, which significantly redistributed stress from within the pressurized region to neighboring locked patches.

Modeling episodic slow-slip events

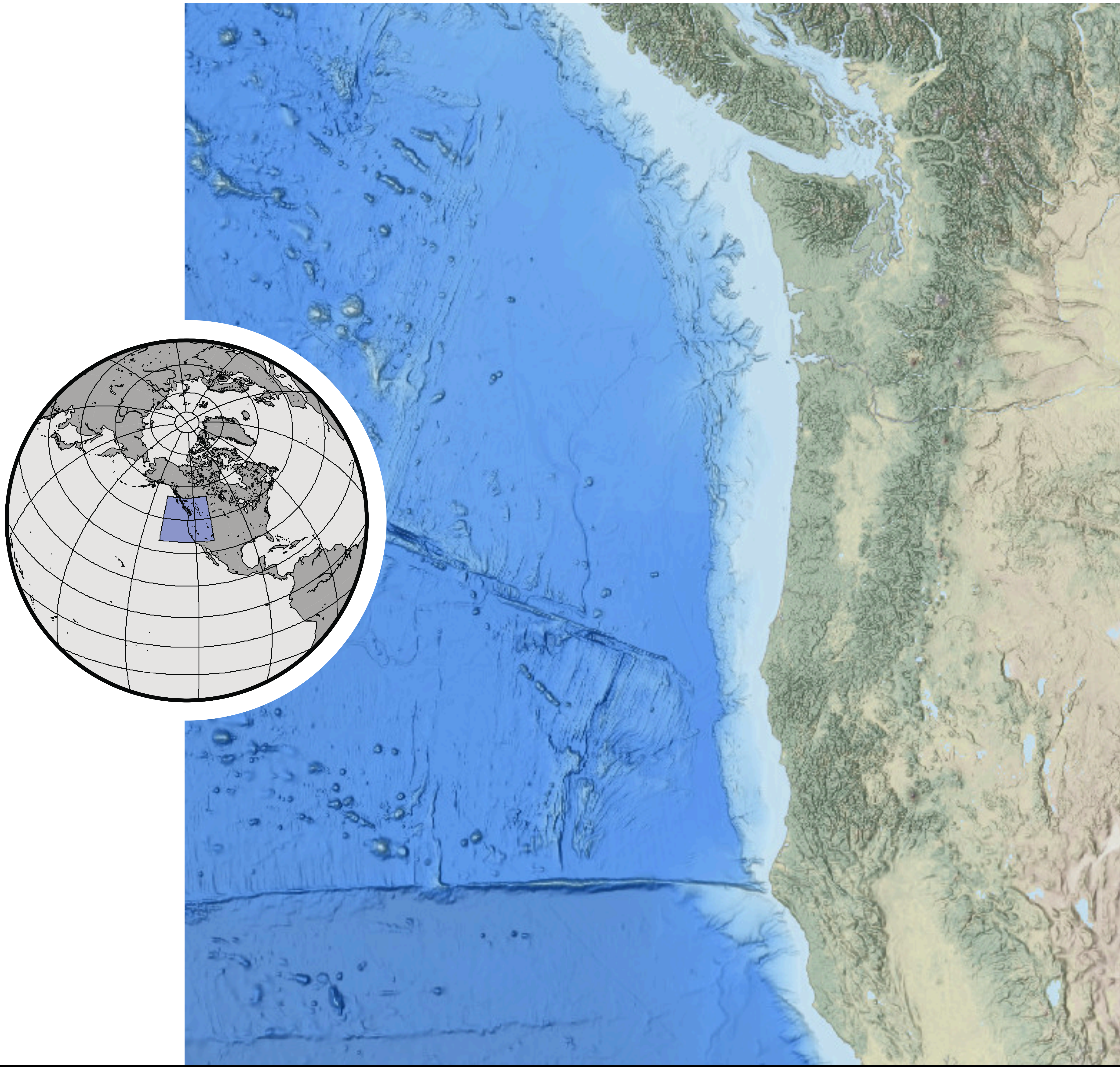

Modeling episodic slow-slip events

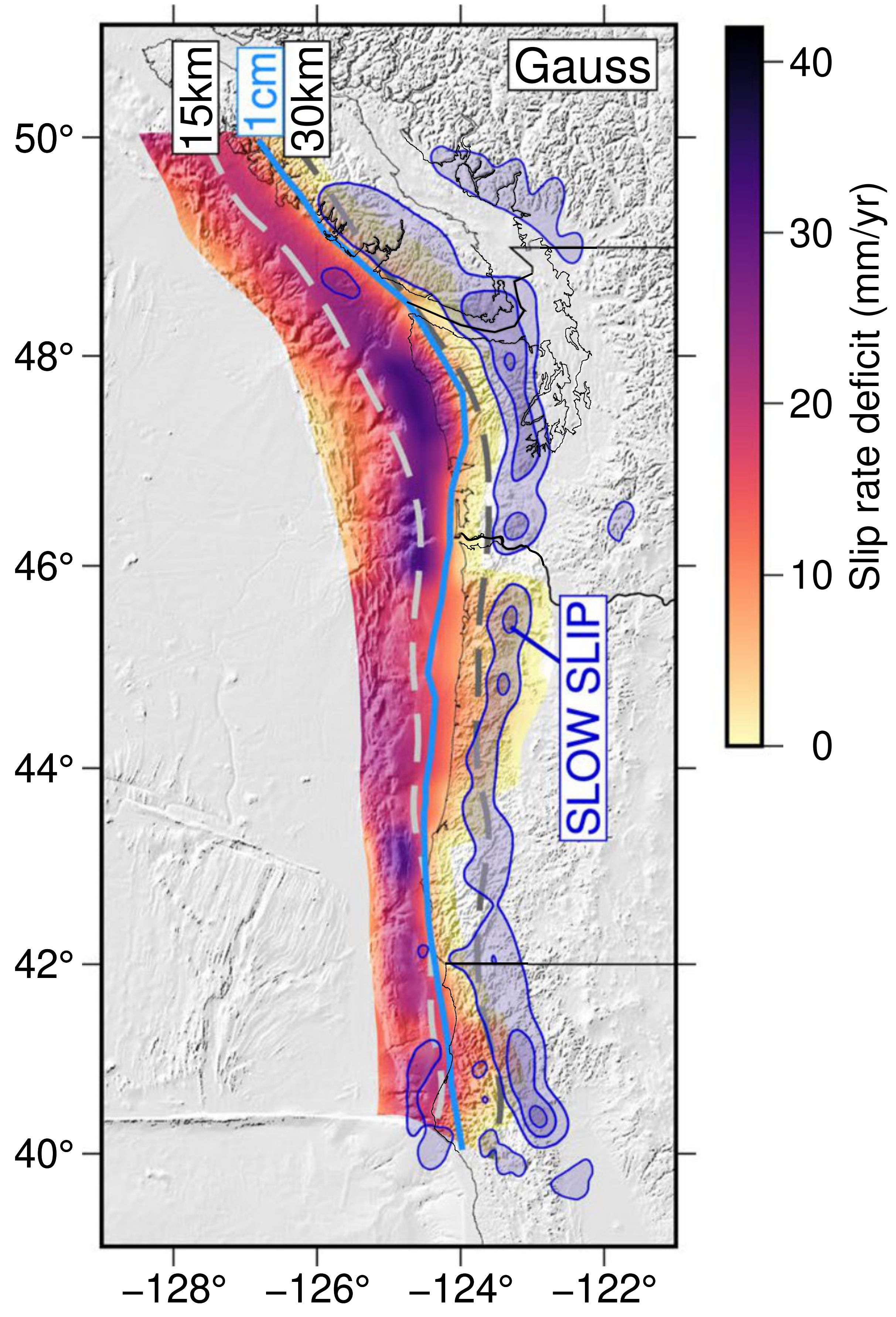

Schmalzle, McCaffrey, Creager (2014)

Li, Wang, Jiang, Dosso (2018)

The most recent **catalog of slow-slip events in Cascadia** contains more than **64 events**. The analysis of this catalog revealed that the slow-slip events propagate with **average rupture speed between ~5.5 and ~11 km/day.**

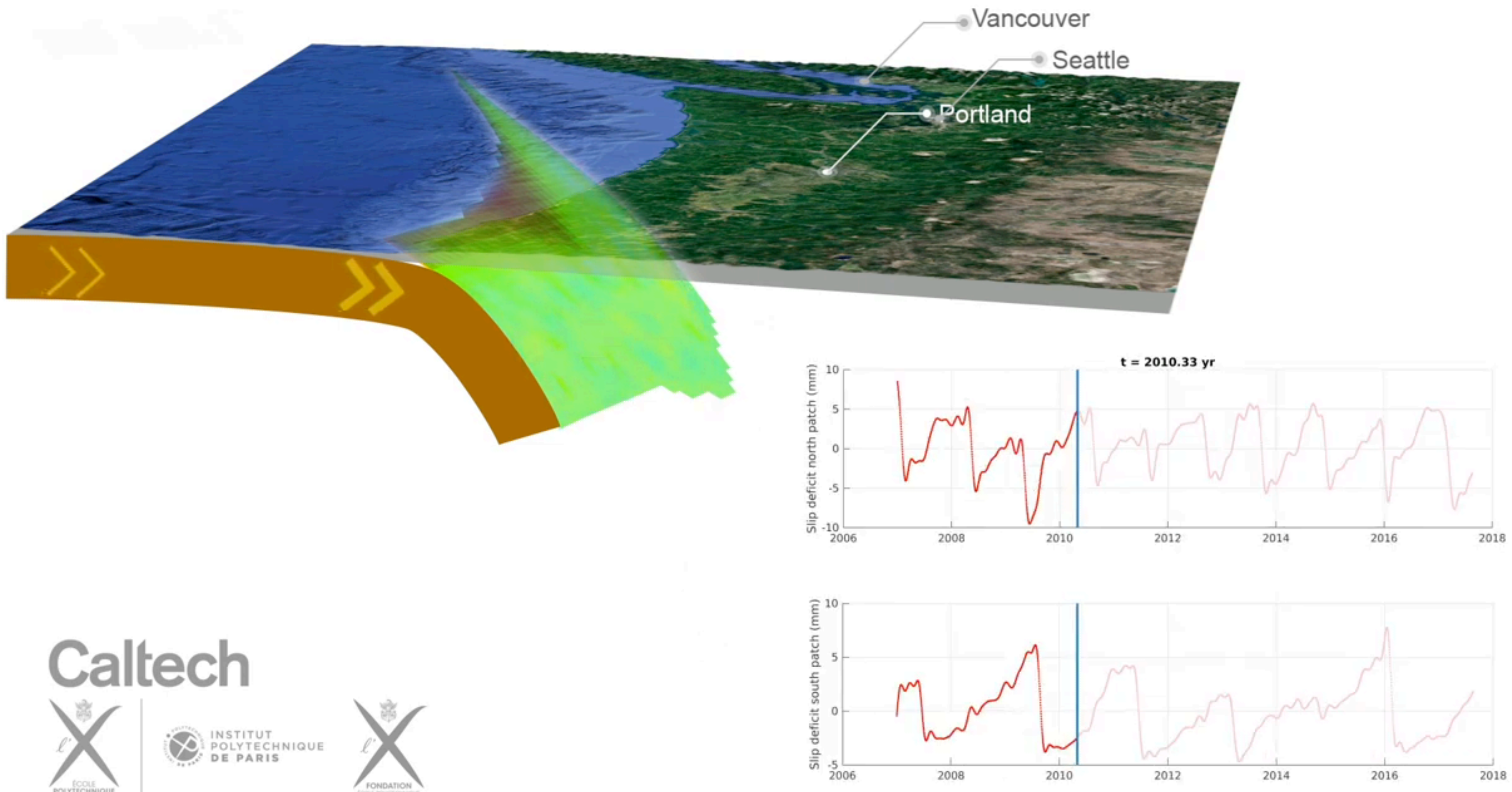

Michel, Gualandi, Avouac (2019)

Moment-Duration scaling

A fundamental characteristic — viewed as a key to unravelling the physical mechanisms of slow and fast rupture — is the **scaling relationship between moment (energy released) and duration.**

A global compilation of SSEs suggests that these events would follow a linear moment duration scaling.

Possible explanation: slow-slip events in Cascadia have very elongated rupture area, suggesting that they might be **geometrically bounded**

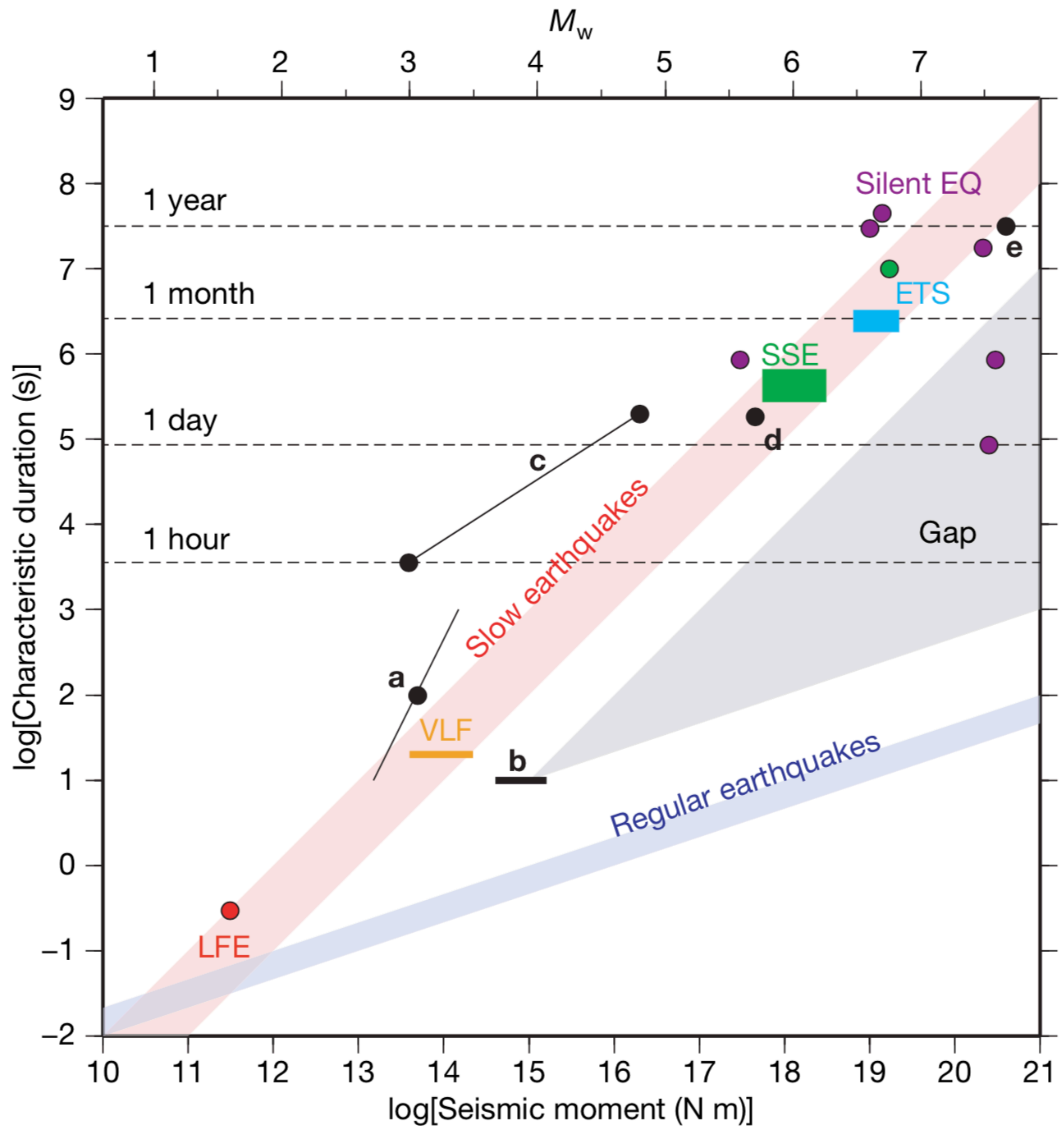

Ide, Beroza, Shelly, Uchide (2007)

Moment-Duration scaling

Regular fast earthquakes have long been known to follow a **cubic moment-duration scaling relation**

Circular crack rupture

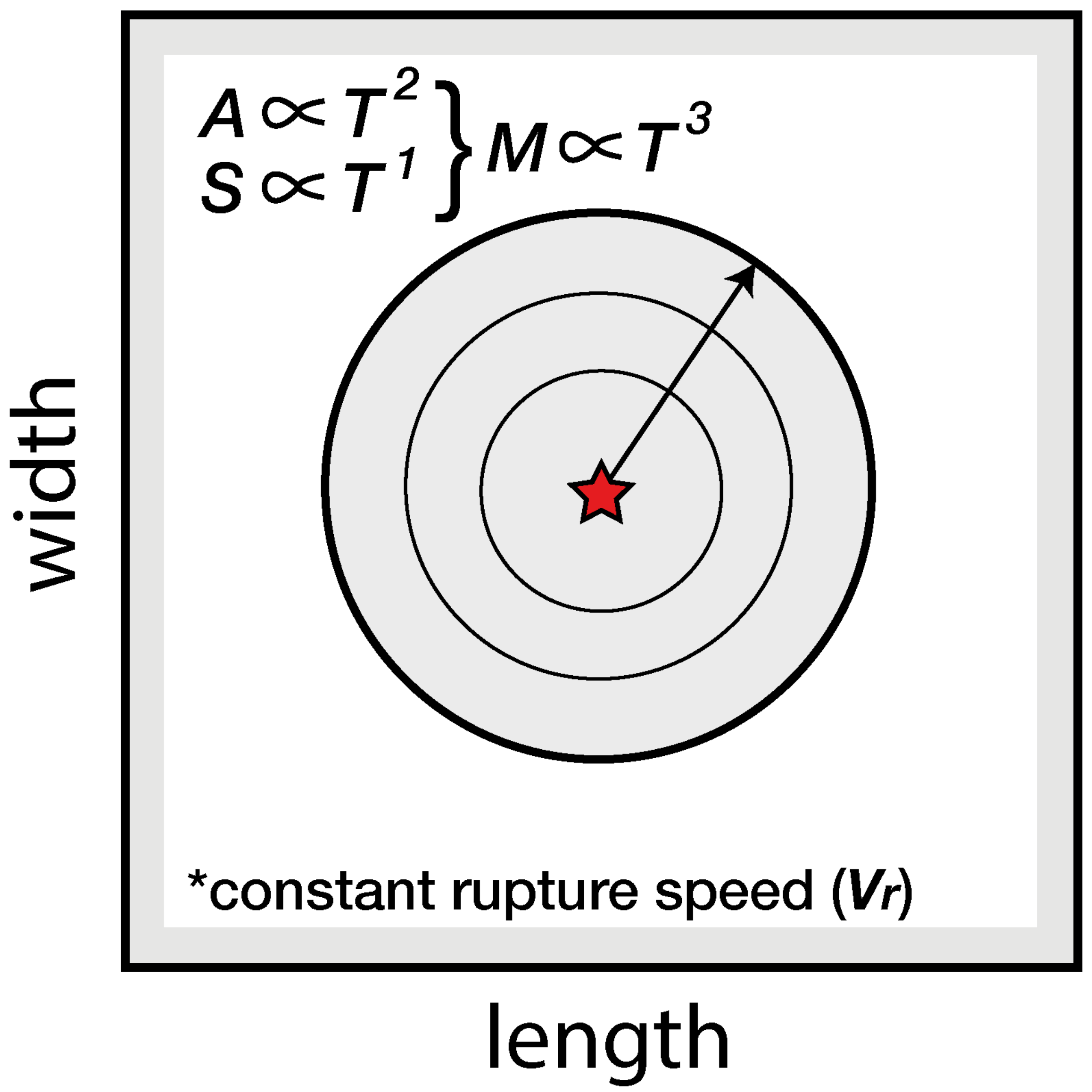

Kanamori and Anderson (1975, BSSA)

The moment-duration scaling should switch to a linear relationship when **slip events saturate the width (W)** of the seismogenic zone

Bounded pulse-like rupture

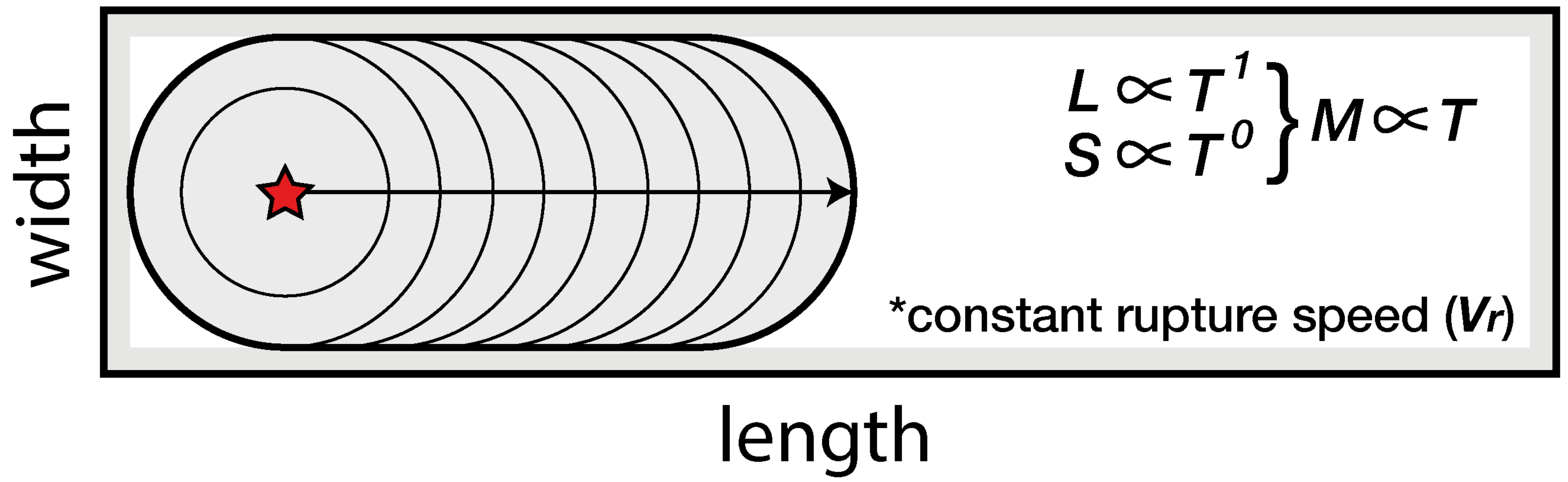

Romanowicz and Rundle (1993, BSSA)

Moment-Duration scaling

The analysis of 10-year-long dataset of slow-slip events from Cascadia and a recent catalog from the Nankai subduction zone suggest that a cubic moment-duration scaling law is in fact more likely.

Furthermore, daily measurement of slow slip from low-frequency earthquakes from the Mexican subduction zone indicate a cubic moment-duration scaling.

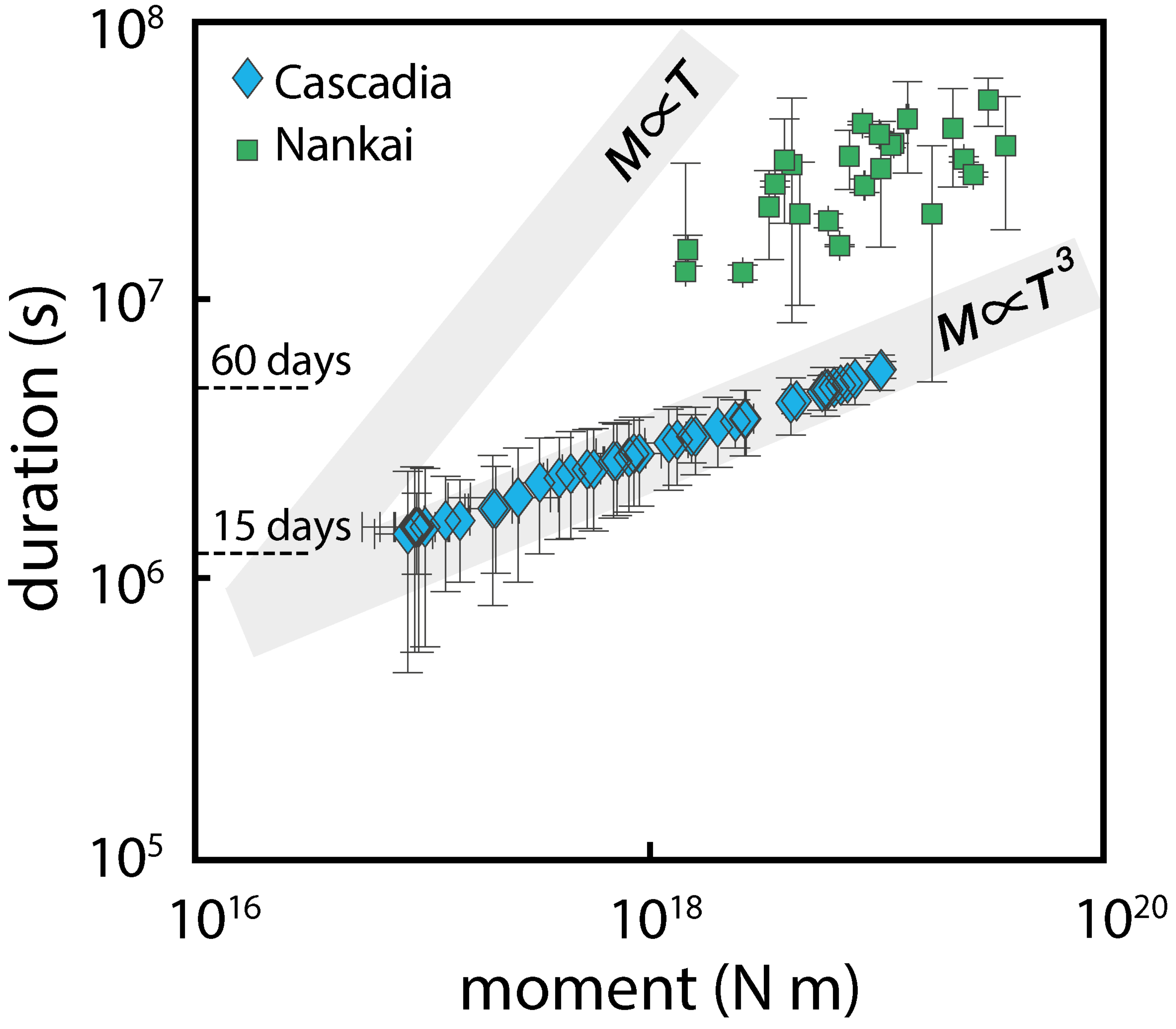

Cascadia, from Michel et al., 2019
Nankai, from Takagi et al., 2019

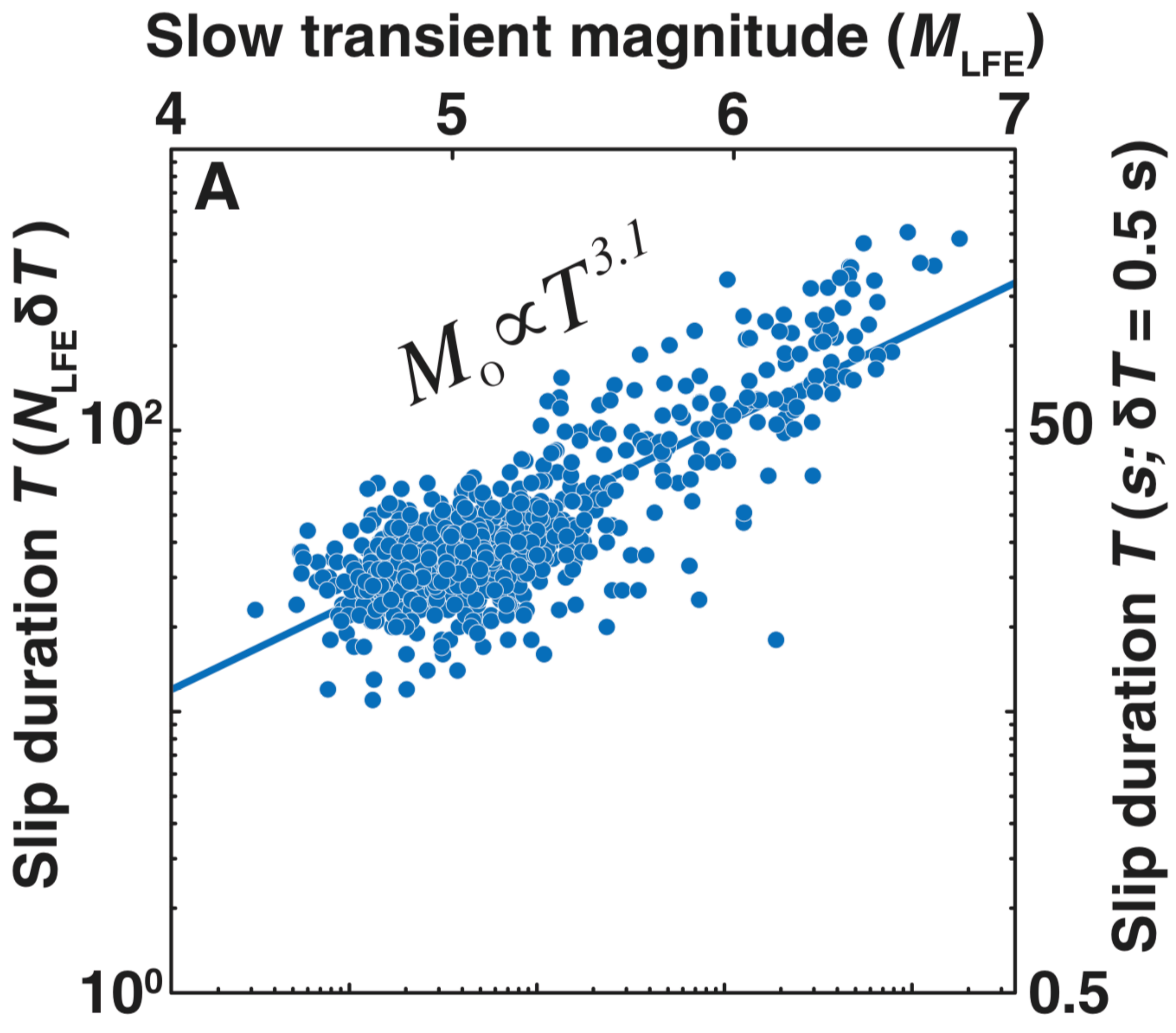

Frank and Brodsky, 2019

Modeling slow-slip events

For numerical simulations of fault slip, we use a Boundary Integral Method (BIM)

The model aims to "mimic" the Cascadia subduction zone:

We consider a thrust fault segment embedded into an elastic medium, loaded by a downdip slip at the long-term slip rate (40

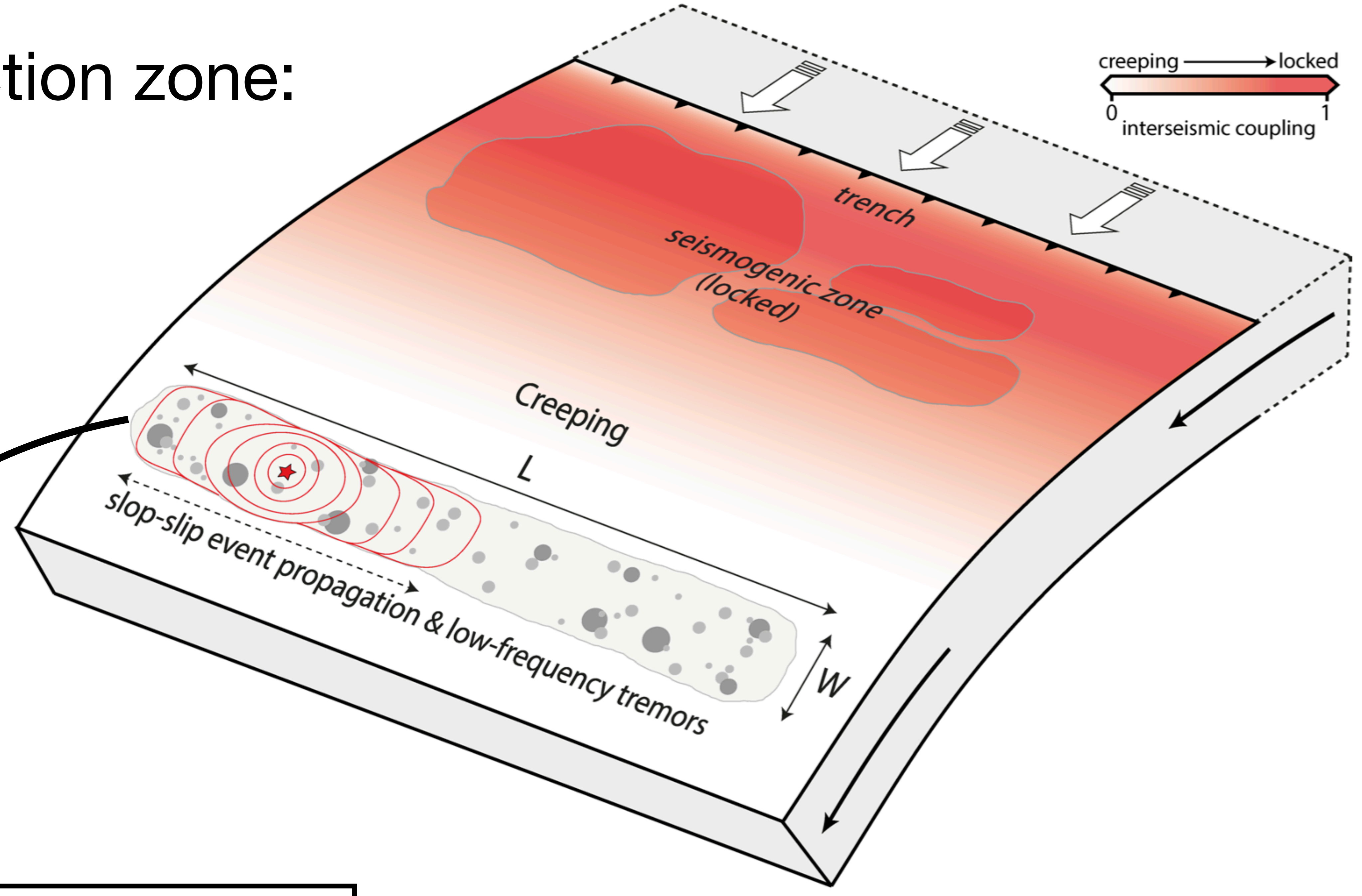

$$\tau = f\,\overline{\sigma} = \left[f^* + a\,ln\frac{V}{V_*} + b\,ln\frac{\theta V}{D_{RS}} \right] (\sigma - p_\mathrm{f})$$

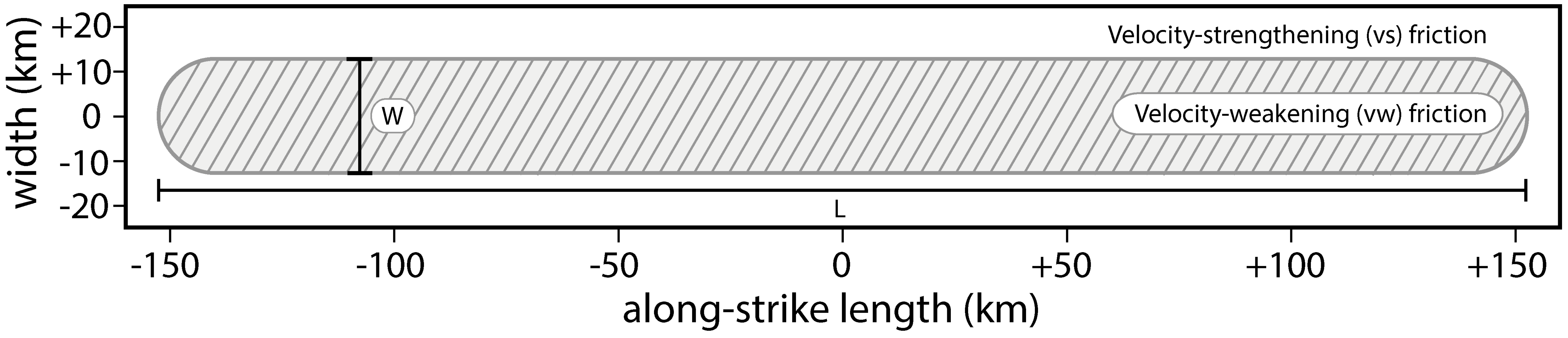

The area with velocity-weakening friction (VW) is embedded in a

Dal Zilio, Lapusta, Avouac (2020)

Dilatancy: shear-induced variations in pore pressure

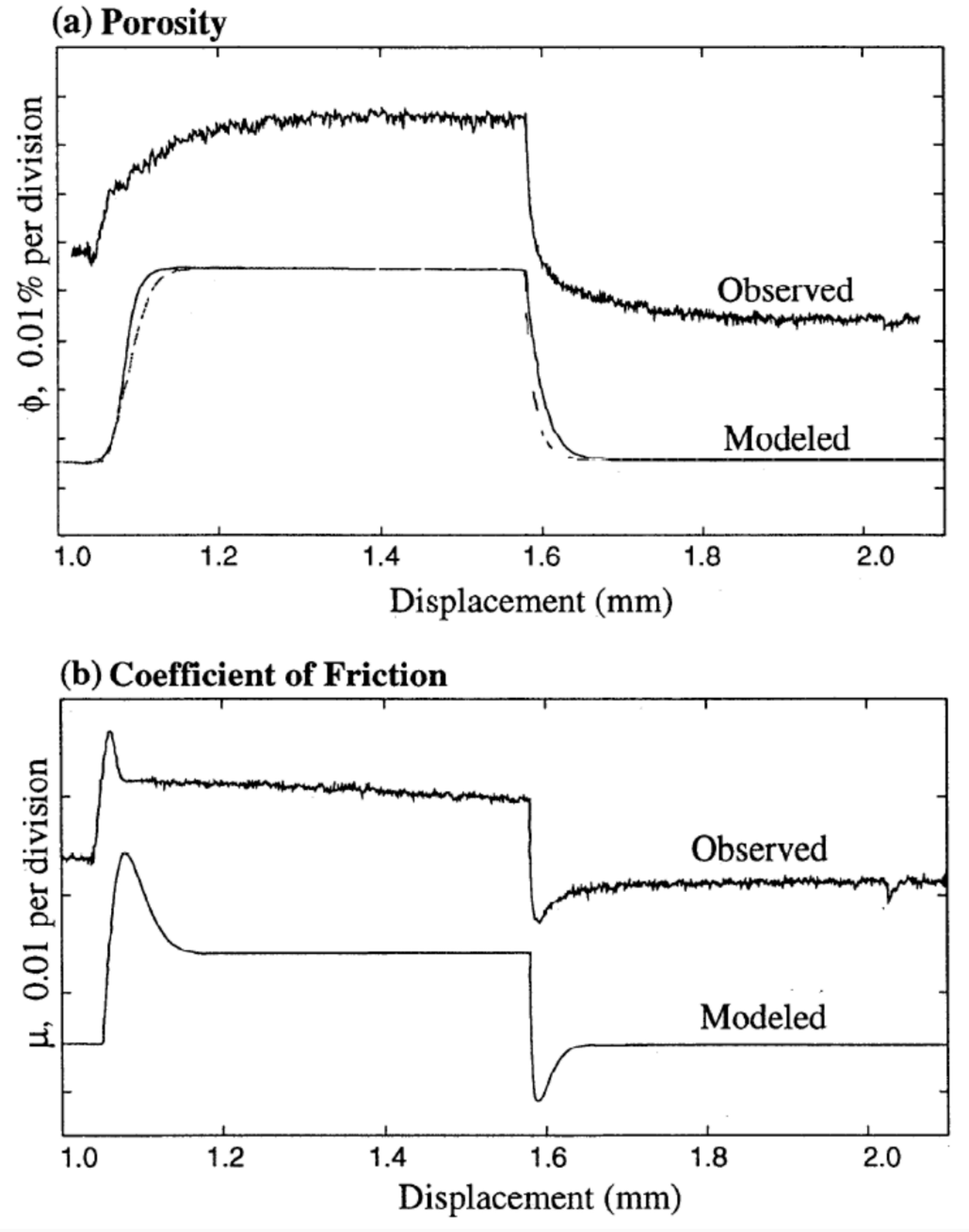

From Segall and Rice, 1995, using experiments of Marone et al., 1990

$$\frac{\partial p}{\partial t} = \alpha_{hy} \frac{\partial^2 p}{\partial y^2} - \frac{F(y)}{\beta} \frac{d\phi}{dt}$$

$$\frac{d\phi}{dt} = -\epsilon \frac{d}{dt} ln \left(\frac{V_0 \, \theta}{D_{RS}} \right)$$

High-pore fluid pressure

The effective compressive normal stress σ is taken to be constant at 10 MPa: this distribution of σ is appropriate for an over-pressurized crust at depth (e.g., Suppe, 2014; Audet et al., 2009; Leeman et al., 2016)

The corresponding elevated pore fluid pressures are required by all friction models to reproduce realistic properties of slow-slip events, e.g.:

(e.g., Liu & Rice, 2005, 2007; Shibazaki & Shimamoto, 2007; Liu & Rubin, 2010; Matsuzawa et al., 2010; Luo & Ampuero, 2018; Viesca & Dublanchet, 2018)

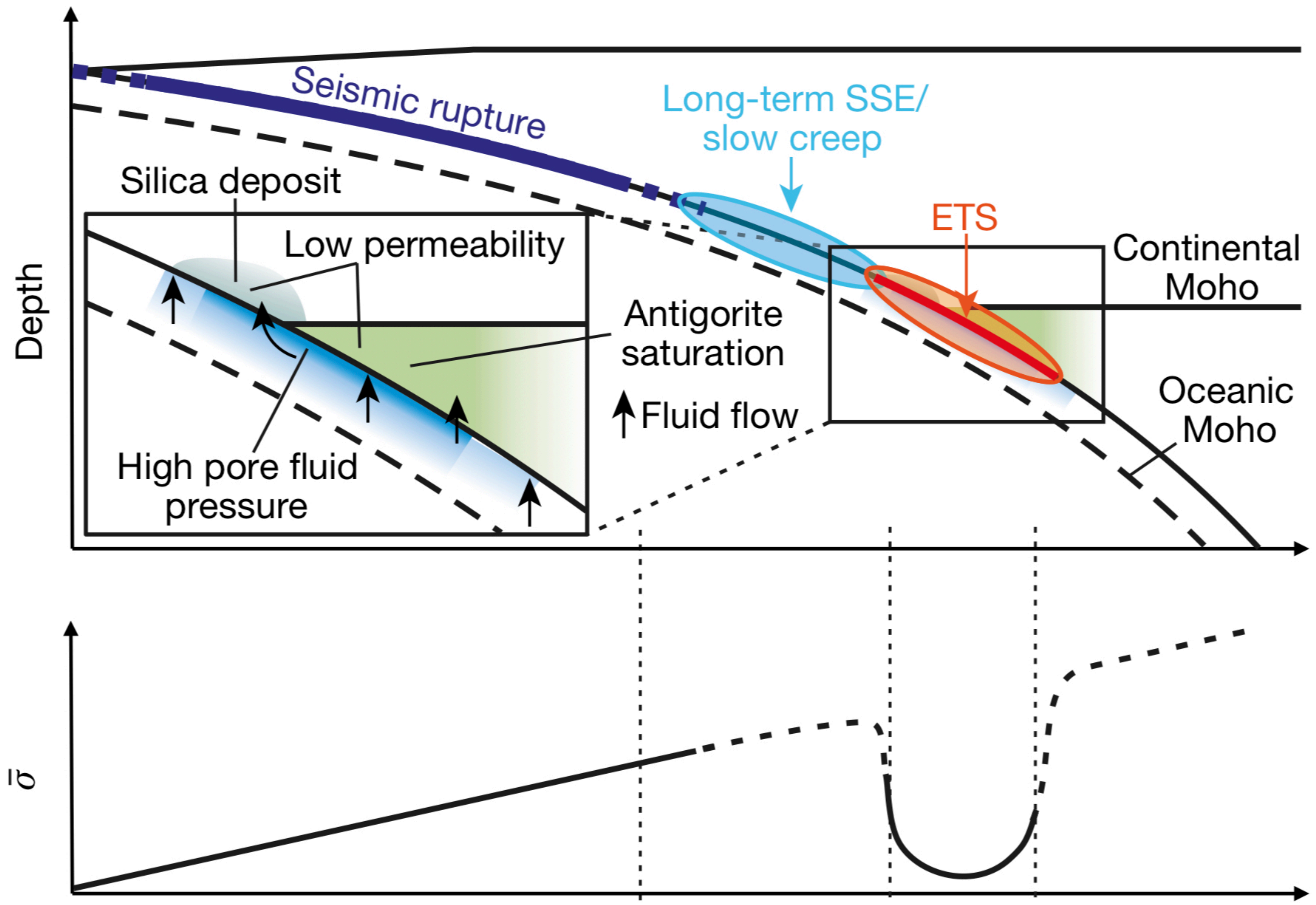

Gao and Wang, 2017

Sequences of slow-slip events

The reference model results in a rich history of SSEs with spontaneous nucleation, slow ruptures, and different sizes

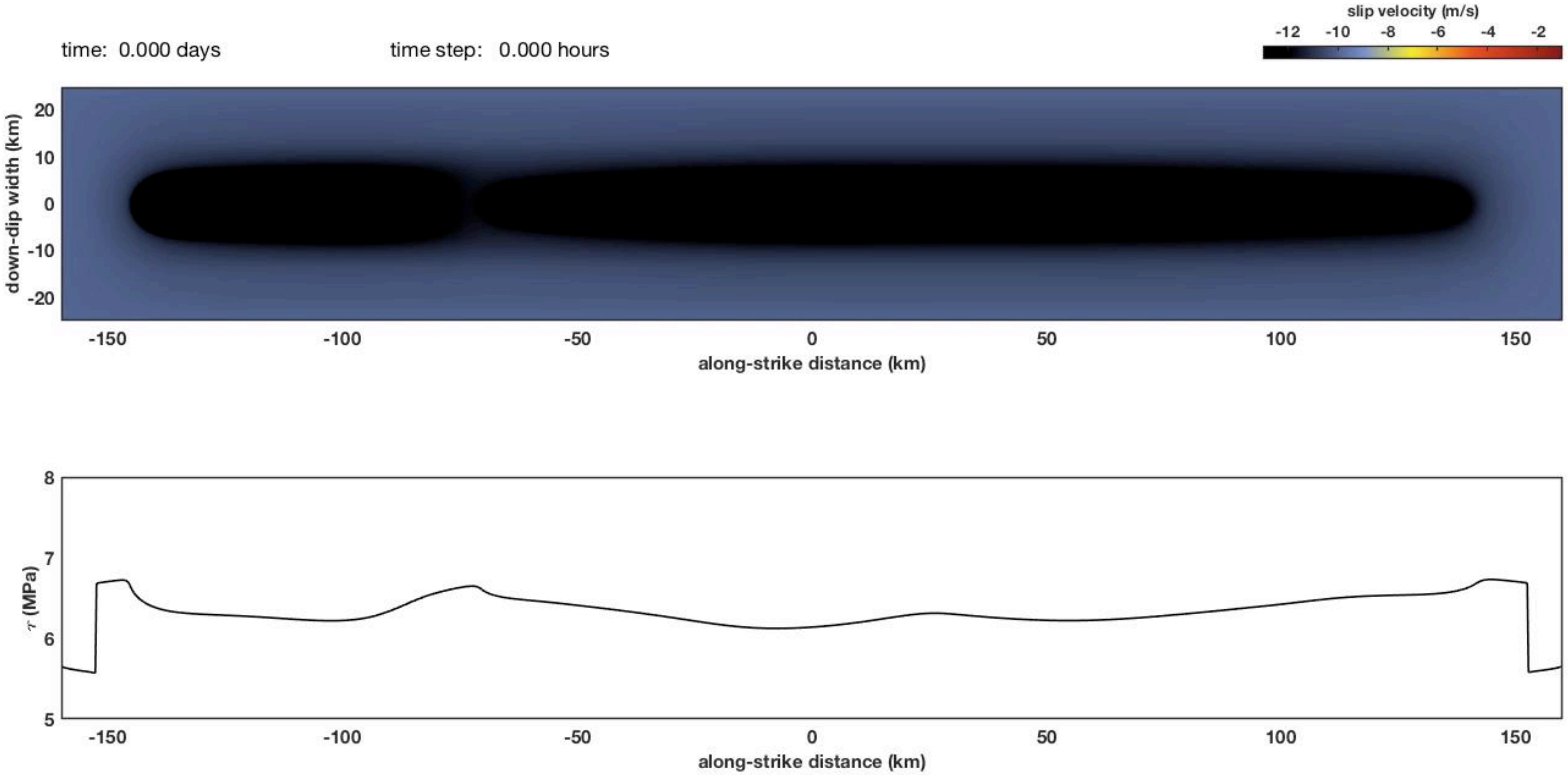

Unraveling the Physics of slow-slip events

Non-constant rupture speed: Rupture front accelerates from ~7.6 to ~9.7 km/day by exploiting a fault patch with a relatively higher pre-stress. It then slows down to ~3.1 km/day and eventually stops in the vicinity of a locked patch

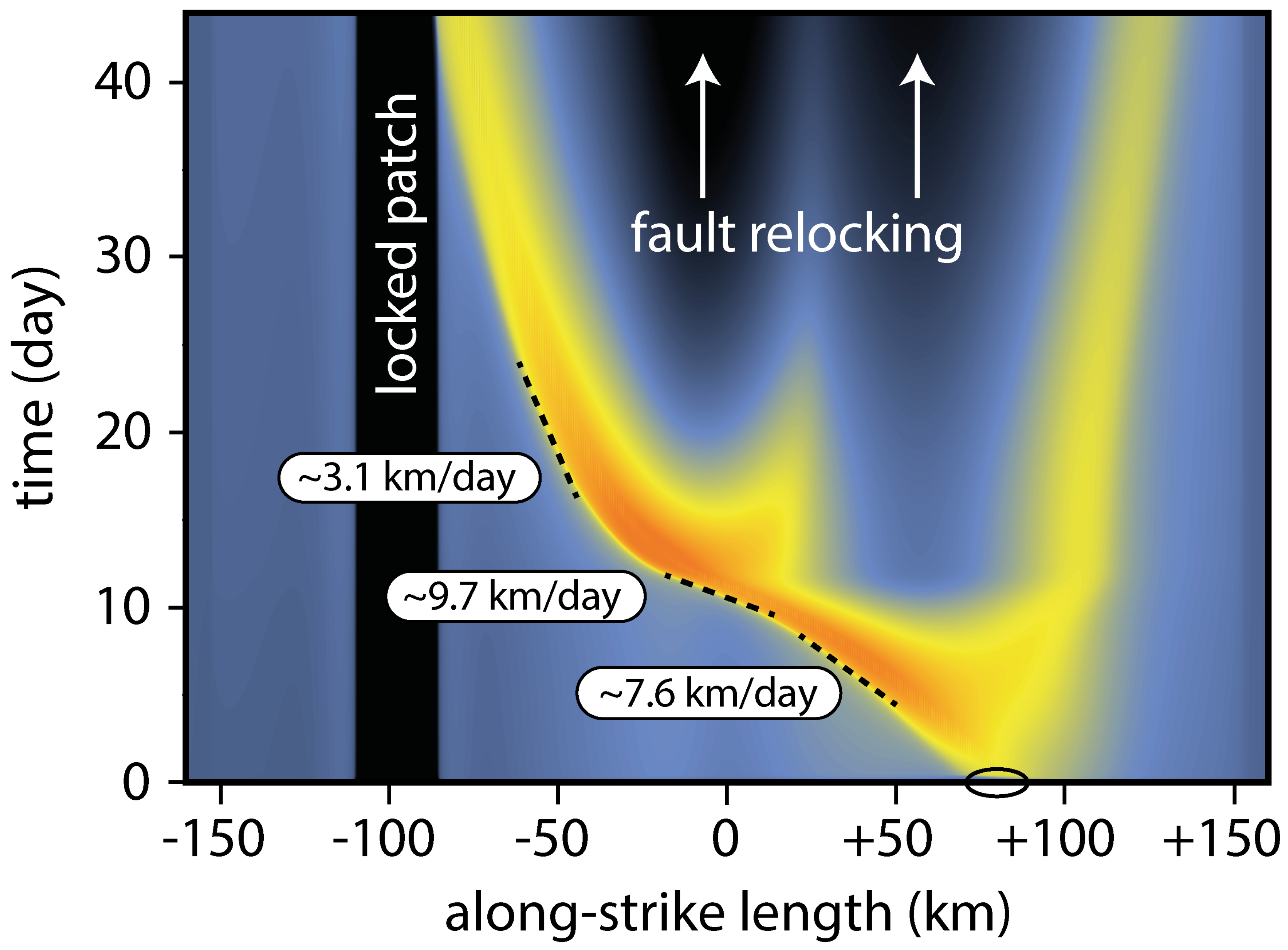

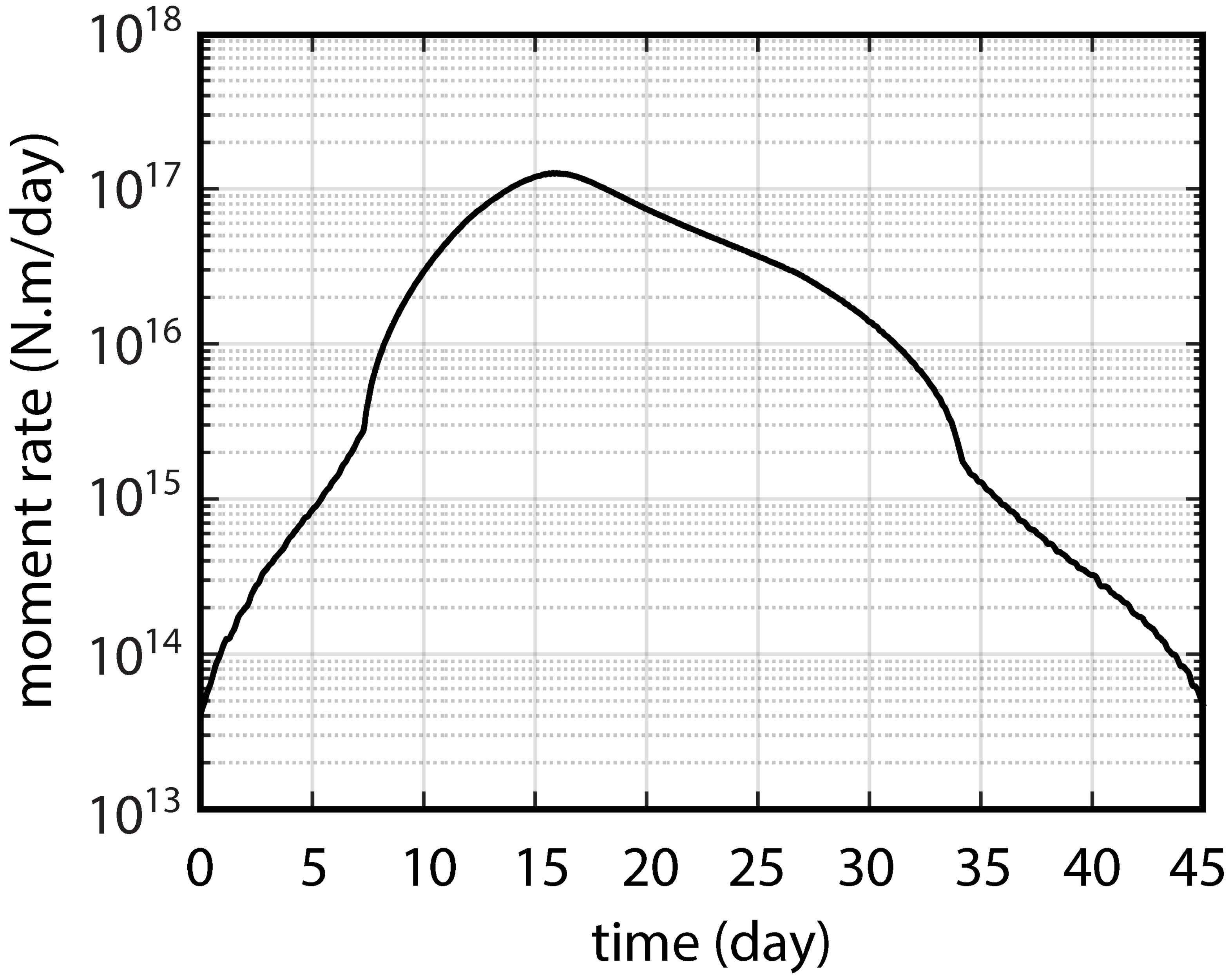

Dal Zilio, Lapusta, Avouac (2020)

Unraveling the Physics of slow-slip events

1. Slip (**S**) scales linearly with the duration (**T**)

2. The final length (**L**) grows and scales with the square of the duration (**T**)

As a results, the **moment released by all events follow a cubic moment-duration scaling law.**

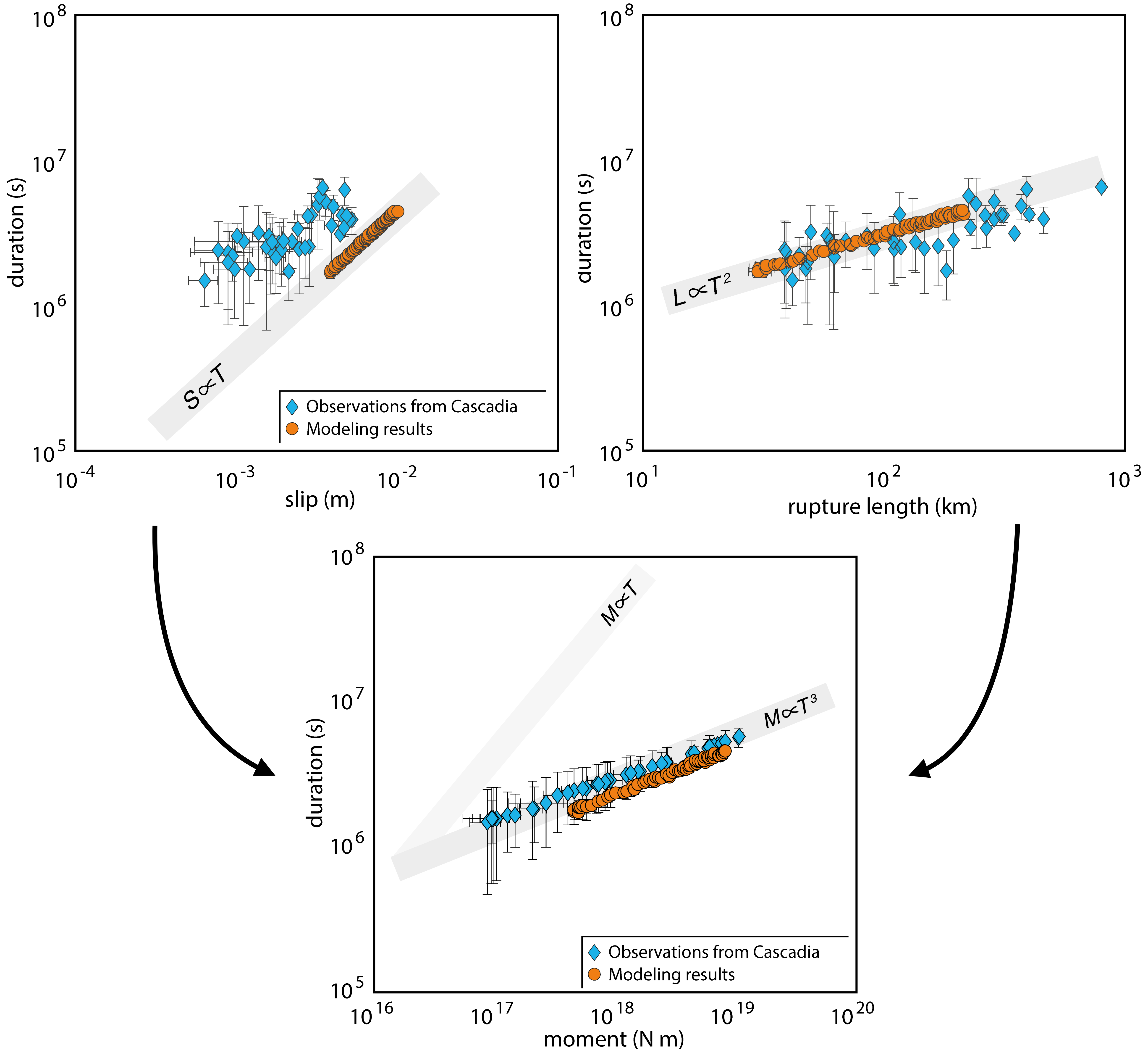

Unraveling the Physics of slow-slip events

Average rupture velocity scales with the size of slow-slip events

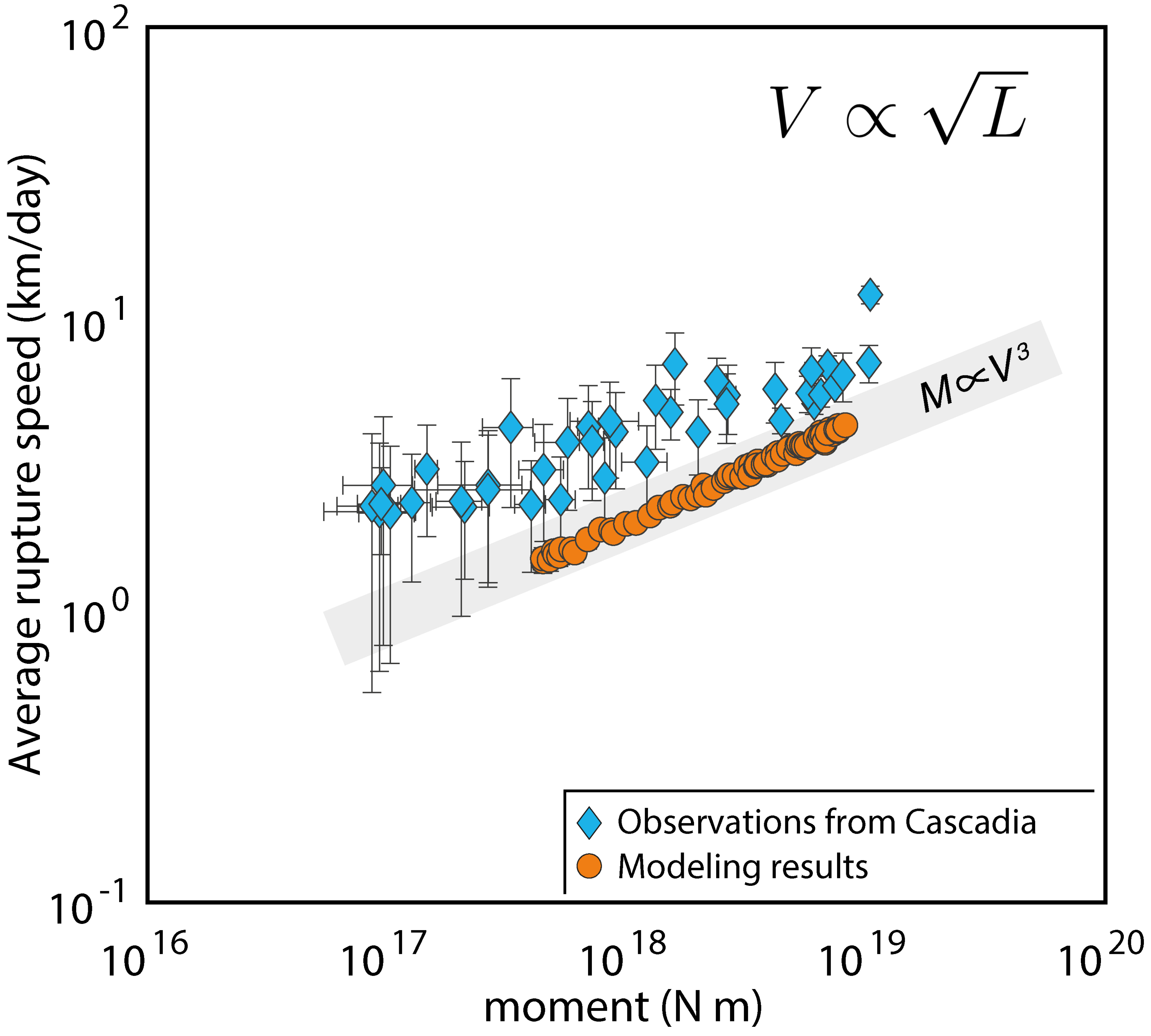

The pulse-like propagation, along-strike segmentation, and frequency-magnitude distribution of our simulated slow-slip events are remarkably similar to those observed on the Cascadia subduction zone (Michel et al., 2018).

However, in contrast to the traditional assumptions, the **cubic moment-duration scaling of slow-slip events arises because the average rupture velocity increases with the increasing magnitude and length of slow-slip events.**

These results highlight the importance of not only determining the moment-duration scaling but also the appropriate explanation for it.